Response to Reviewer's Comments

Manuscript Number: acp-2016-883

Authors: Zhaolian Ye, Jiashu Liu, Aijun Gu, Feifei Feng, Yuhai Liu, Chenglu Bi, Jianzhong Xu, Ling Li, Hui Chen, Yanfang Chen, Liang Dai, Quanfa Zhou, Xinlei Ge

Response to Reviewer #1

General comment: This manuscript reports the measurement results of submicron aerosols by the SPAMS in Nanjing. Recently the Aerodyne AMS has been widely used around the world, and this work presents for the first time the results using the SP-AMS in the YRD region. This is overall a very well written paper with quite thorough analyses of the data, the figures are informative and the results provide new insights regarding the aerosol chemistry in this region.

Authors' reply: We thank the reviewer for his positive comment, and our point-to-point replies to the reviewer's comments are listed below.

The authors assume CO_2^+ = CO^+ in calculating elemental ratios because of the influences of inorganic carbonate. The authors can have a better evaluation of the relationship between CO^+ and CO_2^+ by showing a scatter plot. The reason is 1) the O/C and OM/OC ratios in Figure 2 are relatively close among different seasons, which is not expected as usual; 2) the mass closure analysis in Figure 3 showed a substantially unidentified fraction, particularly in summer. For example, organic aerosol only accounts for 16% of PM2.5 in summer. Is it due to the low OM/OC ratio? In addition, Canagaratna et al. (2015) recommended a new calibration factor for O/C, which can also increase the OM/OC ratio, and hence the total mass of organic aerosol.

Authors' reply: Thanks for the suggestion. First, as recommended, we have tried to make a scatter plot of original CO_2^+ vs. CO+. The plot has a good correlation coefficient of r^2 = 0.92, but is with an abnormally high slope ~2.24. Although a previous study that also used argon as carrier gas for atomization of PM1 samples collected in Europe sites (Bozzetti et al., 2017), also found that the signal of CO_2^+ appeared to be systematically higher than that of CO^+, but the factor is much less than 2.24. Considering the different size cuts of that study and this work, it is indeed very likely that a significant portion of CO_2^+ could be due to carbonate, which is also in

some extent verified by the anion deficiency in Figure 6a. Thus, we believe it is likely reasonable to assume CO_2^+ equal to CO^+, as this ratio is proposed by Aiken et al. (2008), and was widely used and accepted by the AMS community. These discussion are now included in the modified manuscript.

Secondly, compared with the online AMS results, the mass fraction of organic matter was somehow low (~20%). But in fact, this OM fraction is well within the typical range of other mass closure results on $PM_{2.5}$ filter samples, as summarized in Liang et al. (2017). Possible reasons that it is lower than those online results include that online measurement cannot measure some crustal elements and also the nitrate/sulfate in supermicronmeter range.

At last, indeed Canagaratna et al. (2015) has proposed new calibration factors for O/C and H/C ratios, which can increase the OM/OC ratio, and hence the total mass of organic aerosol. In the revised manuscript, we now used the new set of calibration factors, and updated all relevant figures (Fig. 2, Fig. 3 and Fig. S4 in the supplement), tables (Table 4, which is original Table 3) and texts in the manuscript. Indeed, the OM mass fraction increased and the elemental ratios of various PMF factors. Please check the details in the revised manuscript.

Interpretation of the COA factor needs to be cautious. It appears to me that defining this factor as COA is not appropriate although the spectrum has some similarities to the standard spectra of cooking aerosols. One of the reasons is the large contribution of COA in water-soluble organic aerosol (annual average 31.2%), which is much higher than those previously observed in urban cities. Another reason is the extraction efficiency of COA is typically much lower than secondary organic aerosol (Huang et al., 2014).

Authors' reply: We generally agree with the reviewer. For the offline AMS-PMF analyses, due to low time resolution, the factor cannot be justified by investigating its diurnal pattern. The factor was defined as COA mainly due to its low O/C ratios and some similarities with previously reported COA mass spectra. As pointed out by the reviewer, the very high mass fraction of this factor suggests that this factor may include significant contributions from other sources in addition to cooking (we cannot conclude there is no cooking contribution as well). Also, we only analyzed the water-soluble fraction of OA, and COA was in fact has a relatively low extraction、recovery ratio in water, as shown by Huang et al., 2014, Bozzetti et al., 2017 and Xu

et al., 2017, it is indeed not appropriate to assign this factor to COA only. We think it is reasonable to define this factor as a local POA factor, which is a mixture of contributions from anthropogenic sources cooking, coal combustion, industry, etc. Relevant figures and discussions regarding this factor were now updated in the revised manuscript.

3. Check Figure 9.The spectral patterns of ion families and elements should be identical.

Authors' reply: Thanks for the comment. We have checked Fig. 9 (a) and (b) to make them consistent. We also checked WSON because it was calculated from N fraction in WSOA in Fig.9 (b). The average concentration of water-soluble organic nitrogen (WSON) over the sampling period was now 1.16 μg N m^{-3} (83 nmol N m^{-3}), replacing the original value of 1.5μg N m^{-3}(114 nmol N m^{-3}).

Correct “Particular” in the title and abstract.

Authors' reply: Corrected.

Some statements need to be clarified. For example, line 33 – 34, higher nitrate than sulfate does not necessarily indicate traffic emissions although I know the authors want to say that traffic emissions are more important than stationary sources. Also, rephrase the statement in line 111 – 114.

Authors' reply: We have rephrased the corresponding descriptions.

Some linear fittings seem not appropriate to force the intercept to be zero, e.g., Figure 6b (winter) and Figure 7b.

Authors' reply: We have now re-plotted the relevant figures without forcing the intercept to be zero, and also modified relevant discussions. For figure 6b, as we wanted to calculate the overall mass ratio for NO_3^- vs. SO_4^{2-}, so we kept the current fitting by forcing the intercept to be zero.

Response to Reviewer #2

General comments: This manuscript reports results obtained during a long-term measurement campaign performed at Changzhou, China. The authors sampled PM2.5 particles on filters during one year (one month per season) and used a wide range of off-line analytical techniques to determine the concentration and chemical composition of these samples. This is a long and important effort in terms of sampling, off-line analysis and data treatment. Results reported in this manuscript will be of interest for the readers of Atmospheric Chemistry and Physics. I recommend its final publication after the authors address the following comments.

Authors' reply: We thank the reviewer for his positive comment, and our point-to-point replies to the reviewer's comments are listed below.

1) The main issue of this manuscript is the absence of discussion on the uncertainty of the results. Given that the authors used a large set of analytical techniques, they should present their uncertainties in their respective sun-section under 2.2 "Chemical analysis". This is particularly important for a few parameters which are calculated using results from two instruments, such as the concentration of water soluble organic aerosols (WSOA), which is obtained from the TOC analyzer and the OM/OC ratio of the SP-AMS.

Authors' reply: Thanks for the suggestion. Now in Section 2.2, we added a new Table 2 which lists the uncertainties and the detection limits of different analytical techniques used in this study. The measurement uncertainties were typically calculated as 3 times the standard deviation on replicate measurements on blank filters. Note the uncertainty of the OM/OC ratio is 6%, which is reported by Aiken et al. (2008). Also, since the WSOA concentrations were based on two instruments (SP-AMS) and TOC, so the uncertainty of WSOA was calculated as the sum of squares of the uncertainties of OM/OC and WSOC analyses.

Table 2 Summary of species, analytical instruments, uncertainties and detection limits.

Species/Parameters	Analytical instruments	uncertainty	Detection limits
Water soluble ions	Ion chromatography	3.5-7.0%	3-20 μg L^{-1}
Trace elements	ICP-OES	10.3-18.5%	16.3%
OC, EC	Thermal-Optical Carbon Anlyzer	<12%	30-80 ng m^{-3} for OC and 30 ng m^{-3} for EC (Mirante et al., 2014)
WSOC	TOC analyzer	3.4-6.0%	5.0 μg L^{-1}
PAH	GC-MS	20%	2-5μg L^{-1}
OM/OC ratio	SP-AMS	6% (Aiken et al., 2008)	-
WSOA	HR-AMS,TOC	6.9-8.5%	-

2) Section 2.1 “Sampling site and PM2.5 collection”: the authors need to mention here the artifacts related to the filter samplings, in particular the evaporation of semi-volatile compounds during the sampling. This is particularly important for some results presented later, such as the NO3-/SO42- ratio. Indeed, if these species are present under the form of ammonium nitrate and ammonium sulfate (as shown in section 3.2), ammonium nitrate will evaporate faster than ammonium sulfate during the sampling. Therefore, the concentrations of nitrate correspond to a lower limit, the real concentrations should be higher, and the real NO3-/SO42- ratios should also be higher. Another artifact concerns the adsorption of gases, such as volatile organic compounds (VOCs), onto the sampling media and collected particles, which can have an impact on the concentration of particle-bound polycyclic aromatic hydrocarbons (PAHs).

Authors' reply: Thanks for your suggestions. In the revised manuscript Sec. 2.1, we added the description that “Note filter-based measurements are inevitably subjected to various sampling artifacts including evaporation of semi-volatile species, and absorption of gases. Nitrate in the form of ammonium nitrate may have some evaporation loss as it is sensitive to temperature variations during sampling, and absorption of gases may influence the quantification of particle-bound polycyclic aromatic hydrocarbons (PAHs).”

3) Section 2.1 “Sampling site and PM2.5 collection”: according to the wind rose plots presented in Fig. S1, the sampling site was under the influence of different air masses, depending on the season. This important information is not discussed in the section 3 “Results and discussion” and the corresponding sub-sections. Did the authors perform a back trajectory analysis to check where the air masses come from during each sampling period?

Authors' reply: That is a good suggestion. Now in Sec. 3.7, we performed back trajectory clustering analysis using the Hybrid Single-particle Lagrangian Intergrated trajectory (HYSPLIT) model. And relevant discussions were now added in the revised manuscript.

4) Section 2.2.5 “Offline SP-AMS analysis”: it would be interesting if the authors explain here the advantages to use the SP-AMS for off-line analysis of filter samples. This kind of analysis presents several problems compared to on-line measurements: a) it has a much lower time resolution (20 hours in this study, instead of a few minutes), b) the total concentrations and size distributions of the species cannot be directly measured (given that the water extracts must be atomized), and c) it introduces artifacts related to the filter sampling. So what are the advantages of using that instrument for off-line analysis?

Authors' reply: In the first paragraph in Sec. 2.2.5, we added one paragraph. “The Aerodyne AMS is specially designed for online and real-time measurements of the submicron aerosol particles. The instrument has a very fine time resolution thus is powerful in capturing the quick atmospheric processes occurred in real atmosphere. While in this study, we used the SP-AMS for offline filter sample analyses. Compared with the online measurements, there are a few advantages: 1) it can greatly expand the application of AMS because it is often unrealistic to deploy the AMS for very long periods as it requires highly skilled personal to carefully maintain and operate the instrument; 2) for some sites, it is not accessible or not suitable for AMS deployment; 3) AMS analysis of organics can provide more details, for instance the elemental composition, oxidation states, etc., thus can offer useful insights into the origin of OA; 3) offline analyses may introduce artifacts compared with the online measurements,

but on the other hand, it also expands the size range as online measurements were often limited in submicron meter range."

5) Section 2.4 "Source apportionment of WSOA": the authors should say a few words on the robustness of this PMF analysis, given that the dataset contains only 69 samples (67 if the authors discarded two outliers) and corresponds to 20-hours averaged samples.

Authors' reply: Thanks for the suggestion. Regarding the number of samples used in PMF, we agree with the reviewer that in general, inclusion of more samples will provide better PMF results and more scientifically sound interpretation of the sources. Due to practical limitations, unfortunately we were only able to include 67 samples in the PMF calculation. Nevertheless, applications of PMF model on a limited number of samples were also reported previously, and can also provide very valuable insights into the sources and processes of the aerosols. For example, Huang et al. (2014) analyzed about in total 57 samples from 4 cities, and identified different sources during heavy haze formation in China; Sun et al. (2011) analyzed in total 24 samples from 4 sites to elucidate the sources and transformation processes of the water-soluble organic aerosols. In our case, we think our PMF analyses may still be trustworthy and valid, as the identified sources were reasonable as discussed later. Nevertheless, we have added relevant description in the manuscript regarding this caveat raised by the reviewer.

6) Lines 369-372: in addition to cations not measured by ion chromatography, a NH_4^+ measured/NH_4^+ predicted of 0.75 in winter can also simply be due to the presence of acids.

Authors' reply: In fact, as we have calculated the ion balance by using all measured ionic species, this sentence seems to be redundant, we now deleted it.

7) Lines 380-383: in summer, the high temperature may lead to a faster evaporation (not dissociation) of nitrate during the filter sampling. This may explain the lower NO3-/SO42- ratio in summer.

Authors' reply: We replace "dissociation" by "evaporation" in the revised manuscript.

8) Lines 389-391: the authors mention that the sulfur oxidation ratio was higher in summer. However, according to Fig. 6c, the difference with the other seasons does not seem significant.

Authors' reply: Yes, the SOR values in summer were not always higher than those in other seasons. But on average and statistically, it is indeed a bit higher. We have change the sentence to be more accurate "On average, the SOR value appears to be a bit higher in summer…"

9) Lines 538-542: it is surprising to notice that the O/C ratio of organics remained almost constant during the four seasons (Fig. 2), while we could expect higher values in summer due to increased photochemical activities. Can the authors say a few words on this in the manuscript? Among all the results presented in this manuscript (OC/EC ratio, etc.), only a higher sulfur oxidation ratio in summer seems to show increased photochemical activities during that period.

Authors' reply: Our measurement results do show similar O/C ratios of the organics across different seasons. It is likely due to: 1) we determined the water-soluble fraction of OA and the WSOA is typically the fraction with higher oxidation states in all seasons; 2) during summer, the gas-phase oxidation may be enhanced, while in other seasons, other oxidation pathway may dominate (likely aqueous-phase pathway), thus on average, the ambient OA yields similar O/C ratios among different seasons. This also indicates that more investigations are necessary to elucidate the detailed formation mechanism and evolution of OA in this region.

Technical comments:

10) Several correlation coefficients are reported throughout the manuscript. Sometimes, the authors use the Pearson's coefficient r, and sometimes the r^2. It will be better to be consistent and use systematically the same correlation coefficient, either r or r^2.

Authors' reply: We use systematically the same correlation coefficient Pearson's coefficient *r* instead of r^2 in the revised manuscript.

11) When at least two references are given in parentheses, please add a space after the semicolons.

12) Title (also in the supplementary material): "Chemical characterization of fine

particular particulate matter".

13)Line 24: "the fine particular particulate matter (PM2.5) samples".

Authors' reply: Corrected.

14) Line 103: "short-term" is quite vague here. The typical duration of field campaigns with the AMS is approximately one month.

Authors' reply: we deleted the word "short-term".

15) Lines 183 and 446: the authors may mention in the title of these two sub-sections that they are talking about particle-bound PAHs, not about gas-phase PAHs.

Authors' reply: Yes, we have added such information as suggested.

16) Line 276: by which factor were ions with S/N ratios between 0.2 and 2 downweighed?

Authors' reply: The ions with S/N ratios between 0.2 and 2 were downweighted by a factor of 2.

17) Line 301: "Previous studies shows showed that low".

Authors' reply: Thanks, we have corrected this typo.

18) Line 363: actually, the NH4+ measured/NH4+ predicted ratio was first presented by Zhang et al. (2007), and used in tens of papers afterwards, Young et al. (2016) being one of them. Therefore, I would suggest to replace this reference.

Authors' reply: Thanks, we have used the original reference.

20) Figure 7: it would be important to include error bars corresponding to the standard deviations. This is particularly important for the Zn concentration in winter: is this high value due to 1-2 outliers, or do all the samples have a high value?

Authors' reply: Thanks. we added error bars corresponding to the standard deviations in Fig.7.

21) Figure 9: please scale the x-axes of the two panels the same way (either *m/z* 10-100 or 10-120).

Authors' reply: The x-axes are now all 10-100.

References:

Aiken, A. C., Decarlo, P. F., Kroll, J. H., Worsnop, D. R., Huffman, J. A., Docherty, K. S., Ulbrich, I. M., Mohr, C., Kimmel, J. R., Sueper, D., et al., O/C and OM/OC ratios of primary, secondary, and ambient organic aerosols with high-resolution time-of-flight aerosol mass spectrometry. Environ. Sci. Technol. 2008, 42 (12), 4478-4485.

Bozzetti, C., Sosedova, Y., Xiao, M., Daellenbach, K. R., Ulevicius, V., Dudoitis, V., Mordas, G., Byčenkienė, S., Plauškaitė, K., Vlachou, A., et al., Argon offline-AMS source apportionment of organic aerosol over yearly cycles for an urban, rural, and marine site in northern Europe. Atmos. Chem. Phys. 2017, 17 (1), 117-141.

Canagaratna, M. R., Jimenez, J. L., Kroll, J. H., Chen, Q., Kessler, S. H., Massoli, P., Hildebrandt Ruiz, L., Fortner, E., Williams, L. R., Wilson, K. R., et al., Elemental ratio measurements of organic compounds using aerosol mass spectrometry: characterization, improved calibration, and implications. Atmos. Chem. Phys. 2015, 15 (1), 253-272.

Huang, R., Zhang, Y., Bozzetti, C., Ho, K., Cao, J., Han, Y., Daellenbach, K. R., Slowik, J. G., Platt, S. M., Canonaco, F., et al., High secondary aerosol contribution to particulate pollution during haze events in China. Nature 2014, 514, 218-222.

Liang, C., Duan, F., He, K., Ma, Y., Review on recent progress in observations, source identifications and countermeasures of PM2.5. Environ. Int. 2016, 86, 150-170.

Mirante, F., Salvador, P., Pio, C., Alves, C., Artiñano, B., Caseiro, A., and Revuelta, M. A.: Size fractionated aerosol composition at roadside and background environments in the Madrid urban atmosphere, Atmos. Res., 138, 278-292, 2014.

Xu, L., Guo, H., Weber, R. J., Ng, N. L., Chemical Characterization of Water-Soluble Organic Aerosol in Contrasting Rural and Urban Environments in the Southeastern United States. Environ Sci Technol 2017, 51 (1), 78-88.

Chemical characterization of fine ~~particular~~particulate matter in Changzhou, China and source apportionment with offline aerosol mass spectrometry

Zhaolian Ye[1,2], Jiashu Liu[1], Aijun Gu[1], Feifei Feng[1],Yuhai Liu[1], Chenglu Bi[1], Jianzhong Xu[3], Ling Li[2], Hui Chen[2], Yanfang Chen[2], Liang Dai[2], Quanfa Zhou[1], Xinlei Ge[2,*]

[1]College of Chemistry and Environmental Engineering, Jiangsu University of Technology, Changzhou 213001, China

[2]Jiangsu Key Laboratory of Atmospheric Environment Monitoring and Pollution Control, Collaborative Innovation Center of Atmospheric Environment and Equipment Technology, School of Environmental Sciences and Engineering, Nanjing University of Information Science and Technology, Nanjing 210044, China

[3]State Key Laboratory of Cryospheric Sciences, ~~Cold and Arid Regions Environmental and Engineering Research~~Northwest Institute of Eco-Environment and Resources, Chinese Academy of Sciences, Lanzhou 730000, China

*Corresponding author, Email: caxinra@163.com

Phone: +86-25-58731394

Abstract: Knowledge on aerosol chemistry in densely populated regions is critical for effective reduction of air pollution, while such studies ~~haven't~~have not been conducted in Changzhou, an important manufacturing base and ~~polluted~~populated city in the Yangtze River Delta (YRD), China. This work, for the first time, performed a thorough chemical characterization on the fine ~~particular~~particulate matter ($PM_{2.5}$) samples, collected during July 2015 to April 2016 across four seasons in ~~Changzhou~~this city. A suite of analytical techniques were employed to ~~characterize~~measure the organic carbon~~/~~ (OC), elemental carbon (~~OC/~~EC), water-soluble organic carbon (WSOC), water-soluble inorganic ions (WSIIs), trace elements, and polycyclic aromatic hydrocarbons (PAHs) in $PM_{2.5}$; in particular, an Aerodyne soot particle aerosol mass spectrometer (SP-AMS) was

deployed to probe the chemical properties of water-soluble organic aerosols (WSOA). The average $PM_{2.5}$ concentrations were found to be 108.3 μg m^{-3}, and all identified species were able to reconstruct ~80% of the $PM_{2.5}$ mass. The WSIIs occupied about half of the $PM_{2.5}$ mass (~52.1%), with SO_4^{2-}, NO_3^- and NH_4^+ as the major ions. On average, nitrate concentrations dominated over sulfate (mass ratio of 1.21), indicating ~~influences from~~that traffic emissions were more important than stationary sources. OC and EC correlated well with each other and the highest OC/EC ratio (5.16) occurred in winter, suggesting complex OC sources likely including both ~~secondarily formed~~secondary and ~~primarily emitted OA.~~primary ones. Concentrations of eight trace elements (Mn, Zn, Al, B, Cr, Cu, Fe, Pb) can contribute up to ~~6~~5.0% of $PM_{2.5}$ during winter. PAHs concentrations were also high in winter (140.25 ng m^{-3}), which were predominated by median/high molecular weight PAHs with 5- and 6-rings. The organic matter including both water-soluble and water-insoluble species occupied ~~20~~21.5% $PM_{2.5}$ mass. SP-AMS determined that the WSOA had an average atomic oxygen-to-carbon (O/C), hydrogen-to-carbon (H/C), nitrogen-to-carbon (N/C) and organic matter-to-organic carbon (OM/OC) ratios of 0.~~36, 1.~~54, 1.69, 0.11, and 1.~~74~~99, respectively. Source apportionment of WSOA further identified two secondary OA (SOA) factors (a less oxidized and a more oxidized oxygenated OA) and two primary OA (POA) factors (a nitrogen enriched hydrocarbon-like traffic OA and a ~~cooking related~~local primary OA~~).~~ likely including species from cooking, coal combustion, etc.). On average, the POA contribution overweighed SOA (55% *vs.* 45%), indicating the important role of local anthropogenic emissions to the aerosol pollution in Changzhou. Our measurement also shows the abundance of organic nitrogen species in WSOA, and the source analyses suggest these species likely associated with traffic emissions, which warrants more investigations on PM samples from other locations.

带格式的: 字体: 倾斜

1. Introduction

Aerosol particles are ubiquitous in the atmosphere and play important roles in air quality, global climate, biogeochemical cycle, and human health, etc ~~(e.g., Heal et al.,~~

2012;Cao et al., 2012;Hu et al., 2015)(e.g., Heal et al., 2012;Cao et al., 2012;Hu et al., 2015). Aerosol pollution can also influence remote territories via long-range transport. Therefore, atmospheric aerosol has received extensive attentions from the government, public and academia (e.g., Zhang et al., 2007;Jimenez et al., 2009)(e.g., Zhang et al., 2007a;Jimenez et al., 2009). Particularly, much attentions have been focused on fine particles ($PM_{2.5}$, aerodynamic diameters less than 2.5 μm) as they can go deeper into the respiratory system, causing more severe health problems than coarse particles (Anderson et al., 2012). However, as is well known, the concentrations, sources, chemical compositions and formation mechanisms of $PM_{2.5}$ are complicated and can vary greatly with meteorological conditions, seasons and regional/local topography, etc. $PM_{2.5}$ can contain a variety of species, i.e., organic carbon/ (OC), elemental carbon (OC/EC), trace elements, inorganic salts, and various organic species such as polycyclic aromatic hydrocarbons (PAHs)(e.g., Wang et al., 2015)(e.g., Wang et al., 2015). In China, haze pollution occurred frequently in recent years, and a large number of studies regarding the chemical characterization of fine particles were carried out in many locations (Wang et al., 2006a)(Wang et al., 2006a), such as Shanghai (e.g., Wang et al., 2016a;Zhao et al., 2015)(e.g., Wang et al., 2016a;Zhao et al., 2015), Beijing (e.g., Sun et al., 2014;Hu et al., 2016;Sun et al., 2016)(e.g., Sun et al., 2014;Hu et al., 2016;Sun et al., 2016), Nanjing (e.g., Zhang et al., 2016;Ding et al., 2013)(e.g., Zhang et al., 2016;Ding et al., 2013), Lanzhou (e.g., Fan et al., 2014;Xu et al., 2014)(e.g., Fan et al., 2014;Xu et al., 2014), Wuhan (e.g., Huang et al., 2016)(e.g., Huang et al., 2016), and other remote sites (Xu et al., 2015), etc.

域代码已更改

Yangtze River Delta (YRD) region, located in EastEastern China, is experiencing severe atmospheric pollution along with the rapid economic development. Some studies carried out in the YRD investigated different characteristics of the fine aerosols, including the mass loading, composition, hygroscopicity (e.g., Ye et al., 2011;Ge et al., 2015)(e.g., Ye et al., 2011;Ge et al., 2015), size distribution, seasonal variation and, source, formation pathway, and their impacts on visibility and climate (e.g., Wang et al., 2012)(e.g., Wang et al., 2012). However, these studies were mostly limited in Nanjing

~~(e.g., Hu et al., 2012;Wang et al., 2016b)~~(e.g., Hu et al., 2012;Wang et al., 2016b) and Shanghai ~~(e.g., Fu et al., 2012;Qiao et al., 2015;Wang et al., 2012)~~(e.g., Fu et al., 2012;Qiao et al., 2015;Wang et al., 2012). Changzhou, situated in the western YRD region, between Shanghai and Nanjing, is also a major city and an important manufacturing base due to its geographical advantage. The city has an area of about 4374 km^2 with a population of 4.45 million. Due to elevated emissions of various pollutants, the number of hazy days increased over the past few years in Changzhou as well. To the best of our knowledge, no work has been published specifically on chemical characteristics and source apportionment of fine particles in Changzhou. Thus, it is scientifically and practically important to investigate the $PM_{2.5}$ characteristics in order to provide efficient control strategies to reduce the PM pollution ~~in~~for Changzhou.

Among various $PM_{2.5}$ constituents, organic aerosol (OA) is a vital component, accounting for a significant, even dominant fraction of $PM_{2.5}$ in ambient air ~~(Zhang et al., 2007). Thus elucidation of its constituents~~(Zhang et al., 2007a). Thus elucidation of its composition, properties and sources is essential. Apportionment of OA into different sources correctly is a critical step towards enabling efficient air pollution control strategies. Recently, Aerodyne Aerosol Mass spectrometry (AMS) has been used extensively for quantitatively characterizing ambient OA, and the ~~obtained \~~wealthy mass spectral data allows a better source analyses of OA ~~(Canagaratna et al., 2007)~~(Canagaratna et al., 2007). Particularly, positive matrix factorization (PMF), as a standard multivariate factor analysis method, has been widely applied on AMS ~~data sets~~datasets to distinguish and quantify the OA sources ~~(Zhang et al., 2011)~~(Zhang et al., 2011). Many previous studies ~~(e.g., Ge et al., 2012a;Ng et al., 2011)~~(e.g., Ge et al., 2012a;Ng et al., 2011) have deployed the AMS for online field measurements since AMS can provide real-time information on mass concentrations and size distributions of aerosol particles with very fine time resolution ~~(~~(several seconds to minutes). However, up to now, AMS was typically used for ~~short term~~ online ~~measurement~~measurements and only a few studies made efforts to apply it on offline filter ~~samples~~sample analyses and source apportionment ~~(Ge et al., 2014;Daellenbach et al., 2016;Sun et al., 2011a)~~(Ge

et al., 2014;Daellenbach et al., 2016;Sun et al., 2011a;Bozzetti et al., 2017;Mihara and Mochida, 2011;Huang et al., 2014;Xu et al., 2015).

In this study, for the first time, we systematically investigated the chemical characteristics of ambient $PM_{2.5}$ collected in Changzhou nearly across one-year period, providing an overview about the concentrations of $PM_{2.5}$, water-soluble inorganic ions (WSIIs), trace elements, carbonaceous species, water-soluble organic carbon (WSOC), and PAHs ~~in $PM_{2.5}$~~, and the relationships among these components. Seasonal variations of different $PM_{2.5}$ components were also discussed. ~~Further~~Furthermore, we employed an Aerodyne soot particle aerosol mass spectrometer (SP-AMS) ~~(Onasch et al., 2012;Lee et al., 2015;Wang et al., 2016c)~~(Onasch et al., 2012;Lee et al., 2015;Wang et al., 2016c) to investigate the properties and potential sources of OA on the basis of high resolution mass spectra determined by the SP-AMS. Findings from this study also ~~adds~~add knowledge to the framework of Pan-Eurasian Experiment (PEEX) ~~(Kulmala et al., 2015)~~(Kulmala et al., 2015).

2. Experiments

2.1. Sampling site and $PM_{2.5}$ collection

The sampling site was set on the rooftop of a nine-story building inside the campus of Jiangsu University of Technology in Changzhou (31.7°N, 119.9°E), as shown in Fig. 1. This site locates in the southwestern part of Changzhou, surrounded by a residential area, approximately 0.5 km away from an urban street - Zhongwu Road, and has no direct influences from industrial emissions (14.7 km away from the closest industrial plant – Bao Steel). Meteorological parameters including temperature, relative humidity (RH), wind speed (WS), wind direction (WD), and concentrations of gas-phase species such as SO_2 and NO_2 are recorded by the air quality monitoring station inside the campus, which is about 500 ~~m~~meters away from the ~~sampling~~ site. ~~Average~~The average meteorological parameters of four seasons are shown in Table 1. The wind rose plots of different seasons are shown in Fig. S1 in the supplement. The wind speed was generally low in Changzhou (on average, 1.1, 1.6, 0.9 and 0.~~8~~9 m s^{-1} in spring, summer, fall and winter, respectively).

$PM_{2.5}$ were collected onto 90 mm quartz fiber filters (Whatman, QM-A) using a medium volume sampler (TH-150 C, Wuhan Tianhong Ltd., China) with a flow rate of 100 L min^{-1}. The filters, wrapped in aluminum foil, were prebaked at 450 °C for 4 ~~h~~hours prior to sampling. The sampler began to collect particles at 9:00 am and stopped at 5:00 am ~~in~~of the following day, ensuring the duration time for each sample of 20 ~~h~~hours. A total of 69 $PM_{2.5}$ samples were collected ~~in 2015 2016~~: 20 July - 19 August 2015 (summer, 11 samples), 18 September - 25 October 2015 (fall, 23 samples), 7 December 2015~~-~~ - 15 January 2016 (winter, 24 samples) and 1 March - 12 April 2016 (spring, 11 samples).

Before and after sampling, the filters were conditioned under constant temperature (22±1°C) and relative humidity (45±5%) for 48 h and weighted by a microbalance (precision of 0.01 mg). The filters were then wrapped and sealed in aluminum foil envelopes separately, stored in a freezer at −20 °C until ~~analysis to minimize the evaporation loss of volatile components.~~. Note filter-based measurements are inevitably subjected to various sampling artifacts including evaporation of semi-volatile species, and absorption of gases. Nitrate in the form of ammonium nitrate may have some evaporation loss as it is sensitive to temperature variations during sampling, and absorption of gases may influence the quantification of particle-bound polycyclic aromatic hydrocarbons (PAHs).

2.2 Chemical analysis

2.2.1 IC analysis

One quarter of a filter was put into a glass tube and 25 mL deionized water (18.2 MΩ cm^{-1}) was then added. After 15 min ultrasonic extraction, the solution was filtrated through an acetate-cellulose filter with 0.45 μm pore size. Concentrations of the WSIIs in the aqueous extract, including five anions (F^-, Cl^-, NO_2^-, NO_3^-, SO_4^{2-}) and five cations (Na^+, NH_4^+, K^+, Mg^{2+}, Ca^{2+}), were then measured by the ion chromatograph (IC, Dionex ICS-600 for anions and ICS-1500 for cations). The method detection limits (~~MDL~~MDLs) were determined to be 18.0, 7.3, 5.2, 6.3, 11.0, 18.7, 3.3, 4.6, 2.6, and 11.5

μg L^{-1} for F^-, Cl^-, NO_2^-, NO_3^-, SO_4^{2-}, Na^+, NH_4^+, K^+, Mg^{2+} and Ca^{2+}, respectively, and all measured concentrations were above the MDLs. Note the filter blanks were treated in the same way, and all data for the samples reported here were blank corrected, other analyses in the following sections were also blank corrected unless specified. The concentrations of all measured species in $PM_{2.5}$ sample were also converted to μg m^{-3} based on the measured concentrations and the air volume pulled through the filter. The uncertainty of the IC measurements, calculated as three times the standard deviation of replicate measurements of blank filters, is shown in Table 2.

2.2.2 ICP-OES analysis

Another quarter of a filter was cut and placed in a Teflon vessel, digested with 10 mL mixture of HNO_3-HCl (1:1, v:v) in a microwave system (XT-9900A, Shanghai Xintuo Co.) for ~~8 h~~45 minutes. After the digested solution cooled down to room temperature, it was filtered through a 0.45 μm acetate-cellulose filter. The filtrate was then diluted using deionized water to 50 mL, and analyzed using Optima 8000 (Perkin Elmer, USA) inductively coupled plasma ~~atomic~~optical emission spectrometry (ICP-OES) to determine concentrations of eight trace elements (Mn, Zn, Al, B, Cr, Cu, Fe, Pb). It is worth to mention that we also tried to measure the concentrations of other trace elements such as Ti, Ni, Ba, but found they were mostly below the detection limits thus were not included in this work. All samples were determined in a triplicate, and a difference within 5% was considered acceptable. Measurement uncertainties for trace metals were in the range of 10.3 – 18.5%, with an average of 16.3% (Table 2).

2.2.3 OC/EC and WSOC analysis

Analysis procedure of OC/EC was similar to a previous study ~~(Zhao et al., 2015)~~(Zhao et al., 2015) . Briefly, OC and EC were measured by the DRI model 2001 thermal/optical carbon analyzer (Atmoslytic Inc. Calabasas, CA) using a 0.526 cm^2 filter punch ~~from~~for each ~~filter~~sample, following the IMPROVE TOR protocol ~~(Chow et al., 2004)~~(Chow et al., 2004). Filter was measured stepwise at temperatures of 140 °C (OC_1),

280 °C (OC_2), 480 °C (OC_3), and 580 °C (OC_4) ~~in~~under a helium atmosphere, and 580 °C (EC_1), 740 °C (EC_2), and 840 °C (EC_3) ~~in~~under a 2% oxygen/98% helium ~~gas~~ atmosphere. OC is calculated as OC_1~~+~~+ OC_2~~+~~+ OC_3~~+~~+ OC_4~~+~~+ OP and EC as EC_1~~+~~+ EC_2~~+~~+ EC_3~~=~~− OP, where OP is the optical pyrolyzed OC. The detection limit of OC was estimated to be 30-80 ng m^{-3} and EC was ~30 ng m^{-3} based on a previous study (Mirante et al., 2014).

带格式的: 字体颜色: 红色

The WSOC concentrations were determined by a TOC analyzer (TOC-L, Shimazu, Japan~~).~~) using a thermos-catalytic oxidation approach. Instrument details and procedure of the WSOC analysis can be found in our previous work ~~(Ge et al., 2014)~~(Ge et al., 2014)~~.~~

. The MDL was 5.0 μg L^{-1} and measurement uncertainties ranged from 3.4 - 6.0%.

2.2.4 GC-MS analysis for particulate PAHs

Due to the limitation of samples, we only analyzed PAHs for spring and winter samples. The ~~PAHs~~ analysis was conducted following the standard procedure, similar to the work of ~~Szabó et al. (2015)~~Szabó et al. (2015). One quarter of a filter was treated by Soxhelt extraction for 18 ~~h~~hours using 250 mL mixture of *n*-hexane/ethylether (5:1, v/v). To determine the recovery rates, 100 ng of deuterated surrogate standard solution containing naphthalene-d_8 and perylene-d_{12} (o2si, USA) was added into the sample prior to extraction, and the average recovery rates of d_8 and d_{12} were over 90%. The extracts were then concentrated to about 2 mL by a rotary evaporator, purified in a chromatography column (filled with 3 cm deactivated Al_2O_3, 10g silica gel, 2 cm deactivated Na_2SO_4). The column was first eluted with 25 mL *n*-hexane and the eluate was discarded, then elution was carried out using 30 mL dichloromethane/*n*-hexane (1:1,v:v). Samples containing PAHs were again concentrated to about 2 mL by the rotary evaporation. Finally they were condensed to exactly 1 mL under a gentle N_2 ~~stream~~steam in a 60 °C water bath. The extracts are transferred into ampoule bottles and stored in a refrigerator until analysis.

The PAH compounds in the final extracts were analyzed with a gas

chromatography - mass spectrometer (GC-MS) (Agilent 7890-7000B, USA), using a DB-5ms capillary column (30 m×0.25 mm×0.5 μm). The instrument conditions were set as follows: injector at 200 °C; ion source at 230 °C; the column was programmed at 40 °C for 2 min, then increased to 100 °C at a rate of 10 °C min^{-1}, held for 1 min, then increased to 250 °C at 20 °C min^{-1}, and finally held for 3 min at 250 °C. The mass selective detector was operated in the electron impact mode using 70 eV. Multi reaction monitor modes were employed for the identification and quantification of PAHs.

Before sample analysis, calibration standards at a series of concentrations were prepared from aromatic hydrocarbon standard (O2si, USA) containing 18 PAH compounds (1000 mg L^{-1}), which are naphthalene (NaP) ($C_{10}H_8$), acenaphthylene (Acy) ($C_{12}H_8$), acenaphthene (Ace) ($C_{12}H_{10}$), fluorene (Flu) ($C_{13}H_{10}$), phenanthrene (Phe) ($C_{14}H_{10}$), anthracene (Ant) ($C_{14}H_{10}$), fluoranthene (Flua) ($C_{16}H_{10}$), pyrene (Pyr) ($C_{16}H_{10}$), benzo(a)anthracene (BaA) ($C_{18}H_{12}$), chrysene (Chr) ($C_{18}H_{12}$), benzo(b)fluoranthene (BbF) ($C_{20}H_{12}$), benzo(k)fluoranthene (BkF) ($C_{20}H_{12}$), benzo(a)pyrene(BaP) ($C_{20}H_{12}$), Benzo(e)pyrene (BeP) ($C_{20}H_{12}$), benzo(j)fluoranthene (BjF) ($C_{20}H_{12}$), ~~benzo(ghi)perylene~~benzoperylene (BghiP) ($C_{22}H_{12}$), indeno(1,2,3-cd)pyrene (~~InP)~~ (~~$C_{22}H_{12}$~~), and dibenz(a,h)anthracene (~~DBA)~~ (~~$C_{22}H_{14}$~~). These PAHs can be classified by the number of aromatic rings and molecular weights: low molecular weight (LMW) PAHs containing 2- and 3-rings (NaP, Acy, Ace, Flu, Phe, Ant), medium molecular weight (MMW) PAHs containing 4-rings (Flua, Pyr, BaA, Chr) and high molecular weight (HMW) PAHs containing 5- and 6-rings (BbF, BkF, BjF, BaP, BeP, InP, DBA, BghiP) ~~(Wang et al., 2015;Kong et al., 2015)~~(Wang et al., 2015;Kong et al., 2015). The calibration was conducted twice prior to analysis. Identification and quantification of each PAH is based on its retention time and peak areas in the calibration curve and sample curve, and the total PAH concentration (ΣPAH) was calculated as the sum of concentrations of all 18 individual PAHs. Figure S2 shows examples of the GC-MS spectra of a few 18-PAHs standards and two surrogate standards (d_8 and d_{12}).

2.2.5 Offline SP-AMS analysis

The Aerodyne AMS is specially designed for online and real-time measurements of the submicron aerosol particles. The instrument has a very fine time resolution thus is powerful in capturing the quick atmospheric processes occurred in real atmosphere. While in this study, we used the SP-AMS for offline filter sample analyses. Compared with the online measurements, there are a few advantages: 1) it can greatly expand the application of AMS because it is often unrealistic to deploy the AMS for very long periods as it requires highly skilled personal to carefully maintain and operate the instrument; 2) for some sites, it is not accessible or not suitable for AMS deployment; 3) AMS analysis of organics can provide more details, for instance the elemental composition, oxidation states, etc., thus can offer useful insights into the origin of OA; 4) offline analyses may introduce artifacts compared with the online measurements, but on the other hand, it also expands the size range as online measurements were often limited in submicron meter range.

The SP-AMS analysis procedure for offline filters was similar to that of ~~Xu et al. (2013)~~Xu et al. (2013). Briefly, for each sample, 1/4 filter was extracted in 25 mL deionized water. The liquid extracts were aerosolized using an atomizer (TSI, Model 3076), and the mist passed through a silica-gel diffusion dryer, leaving dry particles which were subsequently analyzed by the SP-AMS. Note the SP-AMS was operated with the laser off so similar to other AMS measurements; it measured non-refractory organic species that can vaporize fast at the oven temperature of 600 ^{o}C. The instrument employs the 70 eV electron impact (EI) ion generation scheme, all vaporized species were broken into ion fragments with specific mass-to-charge (*m/z*) ratios, and the time-of-flight mass spectrometer outputs the mass spectrum that records the ions according to their signal intensities ~~and~~at different *m/z* ratios. Ion fragments with *m/z* up to 300 amu were recorded in this study. The SP-AMS mass spectra can well represent the total OA constituents, and the bulk OA properties such as elemental ratios including oxygen-to-carbon (O/C), hydrogen-to-carbon (H/C) and nitrogen-to-carbon (N/C) ratios, and the organic mass-to-organic carbon (OM/OC) ratio can be obtained. Note although the SP-AMS is limited in molecular-level speciation analysis ~~(Drewnick,~~

带格式的: 缩进: 首行缩进: 0.29 英寸

2012)(Drewnick, 2012), some compounds can be identified via recognition of thetheir corresponding fingerprint ions, and particular sources can be separated and quantified via further factor analyses.

The SP-AMS data were processed using the Igor-based software toolkit SQUIRREL (version 1.51H56D) and PIKA (version 1.10H15D) (downloaded from: http://cires.colorado.edu/jimenez-group/ToFAMSResources/ToFSoftware/index.html), and the analysis procedure was similar to our previous work (Ge et al., 2012b)(Ge et al., 2012b). We did some minor modifications on the fragment table. For example, we set the organic CO_2^+ signal equal to organic CO^+, same as Aiken et al. (2008), as the CO_2^+ signal in $PM_{2.5}$ may come from carbonate not organics, and since we used Argon as carrier gas so different from ambient measurements, the CO^+ signal can be well separated and quantified from N_2^+ at *m/z* 28 (example shown in Fig. S3). Note the scatter plot of original CO_2^+ *vs.* CO^+ signals yielded a slope of 2.24. A recent AMS study using argon as carrier gas on PM_1 filter samples also showed systematically higher CO_2^+ signal than CO^+ but much less than the factor of 2.24, indicating that CO_2^+ signal from $PM_{2.5}$ sample was influenced by CO_2^+ from carbonate. Accordingly, organic H_2O^+, HO^+, O^+ were scaled to CO_2^+ using the ratios proposed by Aiken et al. (2008), and the elemental compositions and H/C, N/C, O/C and OM/OC ratios of OA reported in this study were also determined according to the method of Aiken et al. (2008)determined according to the method of Canagaratna et al. (2015).

带格式的: 上标

2.3 Determination of WSOA, WIOA

Mass concentrationconcentrations of water-soluble organic mass (WSOA) were calculated by multiplying the WSOC concentrations determined from the TOC analyzer with the OM/OC ratios calculated from the SP-AMS mass spectra (Fig. 2) (equation 1). As shown in Fig. 2, most OM/OC values were within the range of 1.45-2.13, in consistent with the typical OM/OC ratios observed at other urban sites. However, the O/C and OM/OC ratios have no significant seasonal differences, indicating that the WSOA sources were likely similar.

The water-insoluble organic carbon (WIOC) mass was calculated as the difference between the OC determined by the OC/EC analyzer and the WSOC, and a factor of 1.3 suggested by ~~Sun et al. (2011a)~~Sun et al. (2011a), was used to convert the WIOC mass to the mass of water-insoluble organic ~~matter~~aerosol (WIOA) (equation 2). The total organic ~~matter~~aerosol (OA) was treated as the sum of WSOA and WIOA (equation 3).

$$\mathrm{WSOA} = \mathrm{WSOC} \times OM/OC_{WSOA} \quad (1)$$

~~=~~(= (OC- - WSOC~~)*~~) * 1.3 (2)

OA~~=~~ = WSOA~~+~~ + WIOA (3)

The measurement uncertainty of WSOA was calculated as the sum of squares of uncertainties of OM/OC ratios and WSOC, ranging from 6.9 - 8.5% (Table 2).

2.4 Source apportionment of WSOA

In this work, we used the PMF Evaluation Toolkit v 2.06 ~~(Ulbrich et al., 2009)~~(Ulbrich et al., 2009) and followed the protocol described by ~~Zhang et al. (2011)~~Zhang et al. (2011) ~~to conduct the PMF analyses.~~ to conduct the PMF analyses. Typically, inclusion of more samples can provide better PMF results and more scientifically sound interpretation of the sources. But applications of PMF model on a limited number of samples (much less than 100) were also reported previously (e.g., Huang et al., 2014;Sun et al., 2011a), and proven to be able to provide very valuable insights into the sources of OA.

Prior to PMF execution, the following steps were performed: Data and error matrix for WSOA were first adjusted based on equation 1; ions with low signal-to-noise (S/N~~<~~ ≤ 0.2) were removed, ~~whereas~~and ions with S/N ratios between 0.2 and 2 were downweighted by a factor of 2; Two runs with huge mass loading spikes were removed; all isotopic ions were removed since their signals are not measured directly but scaled to their parent ions. The PMF solutions were explored by varying the factors from 1 to 8 and the rotational forcing parameter (*f*peak) from −1 to 1 with an increment of 0.1. The four-factor solution with *f*peak=0 was chosen as the best solution ~~in this study.~~. The mass spectra of three-factor and five-factor solutions were presented in Fig. S4. The

带格式的: 两端对齐, 缩进: 首行缩进: 0.29 英寸, 孤行控制

带格式的: 字体: +西文正文 (Calibri), 非加粗

带格式的: 缩进: 首行缩进: 0.29 英寸, 孤行控制

three-factor solution does not resolve well the oxygenated OA factors as many oxygenated ions were mixed with the primary OA factors. The five-factor solution splits ~~the cooking-related~~a primary OA factor into two factors with very similar ~~factors based on the spectral patterns~~mass profiles. Also, by investigating the correlations of the factors with their corresponding tracer ions, and sulfate, nitrate, etc., of the 3-, 4-, and 5-factor solutions, the 4-factor solution was found to be the most reliable and representative solution.

3. Results and discussion

3.1 Overview of $PM_{2.5}$ concentrations and components

The annual and seasonal average concentrations of $PM_{2.5}$, OC, EC, OA, WSIIs, trace elements and PAHs are summarized in Table ~~2~~3. As shown in Table ~~2~~3, the $PM_{2.5}$ concentrations (in μg m^{-3}) were on average (±1σ) 106.0 (±24.4), 80.9 (±37.7), 103.3 (±28.2), and 126.9 (±50.4) in spring, summer, fall and winter, respectively, with annual average of 108.3 (±40.8), comparable to the $PM_{2.5}$ concentrations in Nanjing (106 μg m^{-3} in 2011) ~~(Shen et al., 2014)~~(Shen et al., 2014), Tianjin (109.8 μg m^{-3} in 2008) ~~(Gu et al., 2010)~~(Gu et al., 2010) and Hangzhou (108.2 μg m^{-3} in 2004-2005) ~~(Liu et al., 2015)~~(Liu et al., 2015), but lower than that in Jinan (169 μg m^{-3} in 2010) ~~(Gu et al., 2014)~~(Gu et al., 2014). The $PM_{2.5}$ concentrations were highest in winter and relatively low in summer, similar to those found in most cities, such as Tianjin ~~(Gu et al., 2010)~~(Gu et al., 2010) and Hangzhou ~~(Liu et al., 2015)~~(Liu et al., 2015). Previous studies ~~shows~~showed that low concentrations occurring in summer ~~are~~were mainly due to the relatively high boundary layer height, low RH and high temperature ~~(Cheng et al., 2015;Huang et al., 2010)~~(Cheng et al., 2015;Huang et al., 2010). The temperatures and RH values were on average 32.1~~℃~~ °C and 61.1% in summer during the observation period (Table 1). Overall, the daily average concentration of $PM_{2.5}$ during sampling period exceeds 75 μg m^{-3} - the second-grade national air quality standard (NAAQS)(GB 3095-2012), and on some heavily polluted days, the $PM_{2.5}$ mass loadings can even exceed 3 times the NAAQS standard.

~~Table 2 summarizes the concentrations of various species determined in this study.~~ Overall, the reconstructed $PM_{2.5}$ mass estimated by the sum of OA, EC and WSIIs *vs.* gravimetrically determined $PM_{2.5}$ mass were shown in Fig. 3(a-d). The mass proportions of all measured components to the $PM_{2.5}$ mass are illustrated by five inserted pie charts representing four seasons and the whole year, respectively. On average, the quantified species can occupy ~~77.3~~78.6% of the $PM_{2.5}$ mass (note trace elements and PAHs were not included as they were only determined for ~~spring and winter~~partial samples), and the mass closure appears to be better for spring and winter samples. Overall, our results are similar to some previous results, such as in Beijing (68%) ~~(Zhang et al., 2013)~~(Zhang et al., 2013). Details and characteristics of individual components are discussed in the following sections.

3.2 Water soluble inorganic ions

The average concentrations (±σ) of total WSIIs were 66.5 (±17.2), 35.0 (±20.2), 51.0 (±17.2), and 66.8 (±23.6) μg m^{-3} in spring, summer, fall and winter, respectively, with an annual average of 56.4 (±22.9) μg m^{-3}. The level was lowest in summer likely due to the conditions favorable for pollutants dispersion and the wet scavenging ~~on~~of these ions under summer monsoon circulation and precipitation. In total, all WSIIs can account for 62.~~6%, 41.1~~7%, 43.2%, 49.~~0~~3% and ~~50.4~~52.6% of $PM_{2.5}$ ~~mass~~ in spring, summer, fall and winter, respectively, with the annual average WSIIs/$PM_{2.5}$ ~~ratio~~percentage of 52.1%, a little higher than the previously reported value of 45.3% in Handan in 2013 (Meng et al., 2016).

The mass fractions of individual ions to total WSIIs followed the order: NO_3^- (34.2~~%)>~~%) > SO_4^{2-} (31.0~~%)>~~%) > NH_4^+~~(~~ (21.2~~%)>~~%) > Cl^-~~(~~ (6.0~~%)>~~%) > Na^+~~(~~ (3.8~~%)>~~%) > K^+~~(~~ (1.8~~%)>~~%) > Ca^{2+}~~(~~ (1.2~~%)>~~%) > Mg^{2+}~~(~~ (0.3%) > NO_2^- and F^-~~(~~ (0.2%) (Fig. 4b). Secondary inorganic ions including SO_4^{2-}, NO_3^-, and NH_4^+, constitute the majority of ~~total~~ WSIIs (86.4%) (Fig. 4b) with the highest one being NO_3^-. Nitrate and ammonium concentrations displayed distinct seasonal variations - highest in spring (NO_3^-: 26.4 μg m^{-3}, NH_4^+: 14.8 μg m^{-3}), following by winter (24.1 and 13.1 μg m^{-3}), and

带格式的: 字体: 倾斜

域代码已更改

lowest in summer (6.8 and 8.2 μg m^{-3}). On the other hand, as a non-volatile species, sulfate concentrations showed no obvious seasonal differences.

The cross-correlation relationships between different ions can be used to infer their possible common sources. Figure 5 shows the Pearson's correlation coefficients (*r*) between ions for four seasons, respectively. As illustrated, NH_4^+ had good correlations with SO_4^{2-} and NO_3^- (*r*~~=~~ > 0.70), and particularly high *r* values were found in winter (with SO_4^{2-}: *r*~~=~~ = 0.90, with NO_3^-: *r*~~=~~ = 0.96) and summer (with SO_4^{2-}: *r*~~=~~ = 0.98, with NO_3^-: *r*~~=~~ = 0.93), indicating these three ions were mainly present in the form of ammonium nitrate and ammonium sulfate~~ and were all formed secondarily.~~. Moreover, the correlations between Na^+ and Cl^- varied largely with the seasons, poor in summer (*r*~~=~~ = -0.~~192~~19) and winter (*r*~~=~~ = 0.37), indicating different sources for them. For chloride, the annual average Cl^-/Na^+ mass ratio was 1.58, larger than 1.17 in seawater ~~(Zhang et al., 2013)~~(Zhang et al., 2013), indicating the important contributions from anthropogenic activities to chloride (such as coal combustion) in Changzhou, in particular in winter as the content of Cl^- in winter was significantly elevated. By contrast, K^+ and Cl^- have good correlations (*r* of 0.86, 0.76, 0.80 and 0.62 in spring, summer, fall and winter), suggesting that K^+ may co-emit with chloride. According to correlation analysis in Fig. 5, Mg^{2+} and Ca^{2+} had good relations with *r* of 0.58, 0.80, 0.81 and 0.78 in spring, summer, fall and winter, respectively, indicating a similar source likely crustal material for these two ions.

Acidity of $PM_{2.5}$ can be evaluated by AE (anion equivalence) *vs.* CE (cation equivalence), which is calculated by converting the concentrations of anions and cations (μg m^{-3}) into molar concentrations (μmol m^{-3}) using the following equations.

$$AE = \frac{SO_4^{2-}}{48} + \frac{NO_3^-}{62} + \frac{NO_2^-}{46} + \frac{Cl^-}{35.5} + \frac{F^-}{19} \quad (4)$$

$$CE = \frac{NH_4^+}{18} + \frac{Mg^{2+}}{12.2} + \frac{Ca^{2+}}{20} + \frac{K^+}{39} + \frac{Na^+}{23} \quad (5)$$

Figure 6a illustrates the scatter plots of CE *vs.* AE in four seasons. The slopes were 1.18, 1.09, 1.03 and 0.93 in spring, summer, fall and winter, respectively, indicating the particles are generally neutralized. Normally, the ratio of $NH_4^+{}_{meas}$/ $NH_4^+{}_{pred}$, proposed

带格式的: 字体: 倾斜

带格式的: 字体: 倾斜

by ~~Young et al. (2016)~~Zhang et al. (2007b), can be used to evaluate the existing form of NH_4^+ ion. The predicted NH_4^+ ($NH_4^+_{pred}$) was calculated using Equation 6.

域代码已更改

$$\sout{NH_{4\ pred}^{+}=18\times(2\times\frac{SO_4^{2-}}{96}+\frac{NO_3^-}{62}+\frac{Cl^-}{35.5})} \quad NH_{4\ pred}^{+}=18\times(2\times\frac{SO_4^{2-}}{96}+\frac{NO_3^-}{62}+\frac{Cl^-}{35.5}) \quad (6)$$

Figure S5 illustrated the ratio of $NH_{4meas}^+/NH_4^+_{pred}$ in $PM_{2.5}$ during four seasons. As presented, the ratios were 0.95, 0.93, 0.87, 0.75 in spring, summer, fall and winter, respectively, ~~indicating~~again verifying that $(NH_4)_2SO_4$ and NH_4NO_3, NH_4Cl were dominant forms for these ionic species. ~~However, the ratio in winter was only 0.75, much less than 1, revealed that the ionic components of $PM_{2.5}$ in winter were more complicated than those in other seasons, reflecting the probability that $PM_{2.5}$ contains other ions such as organic cations in winter.~~

In addition, the mass ratio of NO_3^- to SO_4^{2-} (NO_3^-/SO_4^{2-}) can be used to ~~identify~~determine whether mobile sources (vehicle) or stationary sources (coal combustion) are dominant for these ions ~~(Wang et al., 2006b~~(Wang et al., 2006b;Arimoto et al., 1996). When the NO_3^-/SO_4^{2-} mass ratio exceeds 1, it means that particle sources at the observation site are likely dominated by mobile sources, while fixed sources play major roles when the ratio is below 1. In this study, the mass ratios of NO_3^-/SO_4^{2-} ~~in sampling site~~ were 1.52, 0.43, 0.99 and 1.29 in the spring, summer, fall and winter, respectively, with an annual average ratio of 1.21 (Fig. 6b). The NO_3^-/SO_4^{2-} ratio varied largely with seasons. Note in summer, a lower NO_3^-/SO_4^{2-} ratio may be also ascribed to high temperature which leads to the ~~dissociation~~evaporation of NH_4NO_3, yet the high NO_3^-/SO_4^{2-} in winter and spring is more likely relevant to traffic emissions from Zhongwu Road near the sampling site (Fig. 1).

Previous studies ~~(Xu et al., 2014)~~(Xu et al., 2014) have indicated that nitrogen oxidation ratio (NOR = $nNO_3^-/(nNO_3^-+nNO_2)$, n refers to the molar concentration), and sulfur oxidation ratio (SOR~~=~~ = $nSO_4^{2-}/(nSO_4^{2-}+nSO_2)$), can be used to estimate the transformation of NO_2 and SO_2 to particle-phase NO_3^- and SO_4^{2-}. The larger SOR and NOR mean more secondarily formed nitrate and sulfate. The seasonal values for SOR

and NOR are plotted in Fig. 6 (c-d). ~~The~~On average, the SOR ~~appears~~value appeared to be a bit higher in summer, indicating that strong photochemical oxidation for sulfate formation, while NOR is relatively higher in spring, suggesting conversion of NO_x into nitrate is more efficient in spring in Changzhou.

3.3 Trace elements

Eight trace elements (Mn, Zn, Al, B, Cr, Cu, Fe, Pb) ~~of the~~for samples collected during fall and winter were determined in this study. The average concentrations (μg m^{-3}) are shown in Fig. 7a. The total concentrations were 6.38 μg m^{-3} and 2.77 μg m^{-3}, accounting for ~~6~~5.0% and ~~3.0~~2.7% of the total $PM_{2.5}$ mass ~~in~~during winter and fall, respectively. These values were relatively higher than those in other cities in China, such as 1.74~~% -~~% - 2.04% in Hangzhou ~~(Liu et al., 2015)~~(Liu et al., 2015). This probably can be explained by re-suspended dust from building construction around the site during the sampling period. In this study, the observed mean levels of trace elements in fall were in the order of Fe>Zn>B>Al>Cu>Mn>Pb>Cr, and ranked in Zn>Fe>B>Al>Cu>Mn>Pb>Cr ~~in~~during winter~~, as demonstrated in~~ (Fig. 7a~~-~~). In fall , Fe accounted for 39.0% of the total trace metal mass, following by Zn (25.6%), B (12.3%) and Al (9.2%), while in winter Zn contributed the largest (53.7%), following by Fe and B. Overall, Fe and Zn were the two most abundant trace elements in $PM_{2.5}$, accounting for over half of the ~~total~~ trace ~~elements~~metal mass. Previous ~~research~~work also found that mass loading of Zn was higher than other elements, even higher than Al in Nanjing in 2013 ~~(Qi et al., 2016). Vehicle exhaust is likely one major contributor to the high concentrations~~(Qi et al., 2016b;Qi et al., 2016a). Vehicle exhaust is likely one major contributor to the high concentration of Zn.

In general, the correlations between various heavy metals are weak, as depicted in Fig. 7b-d, indicating that the complex sources including both natural and anthropogenic sources for the trace metals observed here. For instance, Cr, Cu, Pb, and Zn can be released from lubricating oils, tail pipe emissions, brake and tire wears ~~(Zhang et al., 2013)~~(Zhang et al., 2013); Fe and Mg are primarily crustal elements, while Zn and Cu

are ~~primarily~~mainly from anthropogenic sources. Fe and Al were only moderately correlated (for example, in fall with r=0.74, Fig. 7b~~)~~), showing that they are not from exactly same sources.

3.4 OC and EC

As presented in Table ~~2~~3, the annual average EC concentration in Changzhou was 5.4 μg m^{-3}, close to Nanjing (5.3 μg m^{-3}) ~~(Li et al., 2015)~~(Li et al., 2015) and Tianjin (5.9 μg m^{-3})~~(Gu et al., 2010)~~(Gu et al., 2010), but lower than those in other cities (e.g., 22.3 μg m^{-3} in Beijing ~~(Duan et al., 2012)~~(Duan et al., 2012), and higher than that observed in Shanghai (2.8 μg m^{-3})~~(Feng et al., 2009)~~(Feng et al., 2009). The seasonally averaged OC concentrations were highest in winter (18.3 μg m^{-3}), followed by fall (13.2 μg m^{-3}) and spring (11.2 μg m^{-3}), and lowest in summer (7.9 μg m^{-3}). The annual average OC concentration was 13.8 μg m^{-3}, comparable to those measured in other cities, such as Shanghai (14.7 μg m^{-3})~~(Feng et al., 2009)~~(Feng et al., 2009), and Tianjin (16.9 μg m^{-3}) ~~(Gu et al., 2010)~~(Gu et al., 2010).

The mass concentrations of total carbon (TC, the sum of OC and EC) were 16.0, 12.1, 21.0, 22.3 μg m^{-3} in spring, summer, fall and winter, respectively (Table 2), corresponding mass contributions to $PM_{2.5}$ were 15.0%, 15.0%, 20.3%, ~~17.5%, 19.7%,~~ and ~~20.1~~17.6% with an annual mean of ~~18.1~~17.8%. This value was similar to those measured in other cities in China, such as Jinan (10~~-~~ - 15%)~~(Gu et al., 2014)~~(Gu et al., 2014), Shanghai (15%) ~~(Zhao et al., 2015)~~(Zhao et al., 2015), and other cities (10~~-~~ - 15% in Tianjin, Haining, Zhongshan and Deyang; ~~Zhou et al. (2016)~~Zhou et al. (2016)). ~~Organic matter (~~The OA ~~=WSOA+WIOA(μg m^{-3})~~concentrations exhibited similar seasonal variations as $PM_{2.5}$, and ranked in the order: winter (~~29.6~~31.2±11.49) > fall (~~20.0~~21.6±11.~~6)>~~9) > spring (~~17.8±3~~18.9~~)>~~±4.1) > summer (~~12.9~~14.0±1.~~2~~4). The average mass fraction of OA in $PM_{2.5}$ was ~~20.3% during~~21.5%, and the ~~sampling period.~~ WSOA contributed 77.7% of the total OA mass, similar to the results in Atlanta (approximately 88% in rural Centreville and 77% in urban Atlanta) (Xu et al., 2017).

As illustrated in Fig. 8, the OC/EC ratios varied in different seasons and were largest in winter (5.16) followed by spring (2.38), summer (1.88) and fall (1.75). The largest OC/EC ratio occurred in winter, indicating that secondary organic carbon (SOC) was likely a significant component of $PM_{2.5}$ in winter ~~(Chow et al., 2005)~~(Chow et al., 2005), however, the high OC/EC ratio may be influenced by biomass burning and/or coal combustion emissions during wintertime too. A number of previous ~~works~~studies about the carbonaceous aerosols in the YRD region also showed that highest OC/EC ratio occurred in winter and the ratio was often larger than 2, such as Shanghai (6.35) ~~(Zhao et al., 2015)~~(Zhao et al., 2015), Nanjing (2.8)(Li et al., 2015), in consistent with our current results in Changzhou.

域代码已更改

3.5 Particulate PAHs analysis with GC-MS and SP-AMS

The average concentrations of the 18 individual PAH and total PAHs (ΣPAHs) in winter and spring are listed in Table ~~3~~4. It can be seen that InP (% of total PAHs: 12.6--14.8%), BghiP (10.8--12.3%) and Chr (10.4--11.0%) were the three most abundant PAHs species, followed by BbF (8.69--9.39%), BaP (7.37--8.29%), BeP (5.83--8.61) and BaA (4.53--8.27%). The Σ PAHs in $PM_{2.5}$ were found in the range of 14.0--365.7 ng m^{-3} (mean: 140.25 ng m^{-3}) and 8.9--91.3 ng m^{-3} (mean: 41.42 ng m^{-3}) ~~in~~during winter and spring, respectively. The ΣPAHs concentrations in this study are higher than those reported in Zhenzhou (39 and 111 ng/m^3 in spring and winter)~~(Wang et al., 2014)~~(Wang et al., 2014) and Shanghai (13.7 ng m^{-3} in spring) ~~(Wang et al., 2015)~~(Wang et al., 2015), but lower than that reported in ~~many sites of~~ Liaoning Province (75--1900 ng m^{-3}) ~~(Kong et al., 2010)~~(Kong et al., 2010). PAHs with medium (4 rings) and high molecular weights (5--6 rings) (MMW and HMW) ~~accounted for~~occupied the majority of PAHs (88.9% in winter and 79.4% in spring). It is well known that MMW and HMW PAHs are usually associated with coal combustion and vehicular emissions ~~(Wang et al., 2015)~~(Wang et al., 2015). Prior study in Nanjing ~~(He et al., 2014)~~(He et al., 2014) also showed the significant contribution of traffic exhaust to some PAHs including BbF, Chr, Flu, InP, BeP, and BghiP, which in total accounted for more than 53% of the total PAHs.

The diagnostic ratios of selected PAHs including Phe/(Ant+Phe), BaP/BghiP, Flua/(Flua+Pyr), BaP/(BaP+Chr) and Phe/(Ant+Phe) can be used to further distinguish the emission sources of PAHs ~~(Szabó et al., 2015)~~(Szabó et al., 2015). As suggested previously ~~(Feng et al., 2015;Saldarriaga Noreña et al., 2015)~~(Feng et al., 2015;Saldarriaga-Noreña et al., 2015), traffic source was characterized with a ratio of BaP/BghiP>0.6, and ratios of Flua/(Flua+Pyr) <0.4, 0.4-0.5, >0.5 ~~indicate~~suggest sources of petrogenic, fossil fuel combustion and coal/wood combustion, respectively. In this work, the Bap/BghiP of 0.61 (winter) and 0.76 (spring) and Flua/(Flua+Pyr) ratios of 0.47 (winter) and 0.50 (spring), all suggest that local vehicular/fossil fuel combustion emissions could be a prominent contributor to particulate PAHs~~ in Changzhou~~, and contribution from long-range transport was thus minor. Meanwhile, BaP/(BaP+Chr) ratio of 0.40 (winter) and 0.44 (spring) also ~~points~~point to the source ~~from~~of gasoline emission ~~(Khalili et al., 1995)~~(Khalili et al., 1995). However, the Phe/(Ant+Phe) ratio of 0.89 (winter) and 0.86 (spring) indicate the coal combustion might be also an important source of PAHs.

On the other hand, by using the SP-AMS, we also identified a series of PAH ions, i.e., $C_{16}H_{10}^+$ (*m/z* 202), $C_{17}H_{12}^+$ (*m/z* 216), $C_{18}H_{10}^+$ (*m/z* 226), $C_{18}H_{12}^+$ (*m/z* 228), $C_{19}H_{12}^+$ (*m/z* 240), $C_{19}H_{14}^+$ (*m/z* 242), $C_{20}H_{10}^+$ (*m/z* 250), $C_{20}H_{12}^+$ (*m/z* 252), $C_{21}H_{12}^+$ (*m/z* 264), $C_{21}H_{14}^+$ (*m/z* 266), $C_{22}H_{12}^+$ (*m/z* 276), $C_{23}H_{12}^+$ (*m/z* 288), $C_{23}H_{14}^+$ (*m/z* 290), $C_{24}H_{12}^+$ (*m/z* 300), $C_{24}H_{14}^+$ (*m/z* 302), $C_{25}H_{16}^+$ (*m/z* 316), $C_{26}H_{14}^+$ (*m/z* 326), and $C_{26}H_{16}^+$ (*m/z* 328~~), as proposed by Dzepina et al. (2007), confirming the existence of PAHs in ambient particles in Changzhou.~~)(Dzepina et al., 2007). Note many PAH ions identified by the SP-AMS were not measured by the GC-MS, and the PAH compound DBA which is determined by the GC-MS was not detected by the SP-AMS. This reflects the different sensitivities and responses to the particle-bound PAHs of these two techniques. Table 45 shows the correlation (*r*) coefficients of the concentrations of a few selected PAHs, and the mass ratios of their concentrations measured by both the GC-MS and SP-AMS (results for SP-AMS were based on measurements of all samples, while results for GC-MS were for 23 samples in winter and spring). It can be seen that the

concentrations of GC-MS-determined PAHs correlated very well with each other (r~~>~~ ≥ 0.92), while the mass loadings determined by the SP-AMS correlated relatively weak. Also, the mass ratios determined from these two instruments were ~~also~~ different. The inconsistencies may be due to the following reasons: (1) ~~the~~ SP-AMS ~~break~~broke the parent PAH molecules into fragments due to 70 ev EI, thus concentration of a specific PAH ion from the SP-AMS cannot represent its corresponding parent PAH compound, while GC-MS ~~determines~~determined the concentration of ~~the~~ molecular PAH compound; (2) One PAH ion in the SP-AMS HRMS may be combination of a few PAHs compounds with the same molecular weights; (3) Sensitivities and responses to the ~~trace amount of~~different PAHs of the SP-AMS may be different, thus may lead to uncertainties of the PAHs quantification. Nevertheless, combining GC-MS and SP-AMS to improve the PAH measurements by the SP-AMS is valuable, and will be the subject of our future work.

3.6 Source apportionment of WSOA

3.6.1 WSOA mass spectral profile

To gain further insights into the particulate OA characteristics, we performed the SP-AMS analyses on the water extract of the $PM_{2.5}$ samples, with a focus on OA. The averaged high resolution mass spectra (HRMS) of WSOA classified by six ion categories and five elements are shown in Fig. 9, and the corresponding inset pie charts represent the mass percentages of the ion families and elements, respectively. As illustrated in Fig. 9a, the $C_xH_y^+$ ion family accounts for ~~38.7~~386.2% of the WSOA HRMS, followed by ~~$C_xH_yO_2$~~$C_xH_yO^+$ (28.~~0~~5%), $C_xH_yN_p^+$ (17.7%) and ~~$C_xH_yO^+$~~ (~~10.4~~$C_xH_yO_2^\pm$ (11.2%). It is worth to mention that we found that the $C_xH_yN_p^+$ ions contributed significantly, and the organic N (ON) could occupy ~~8~~6.4% of the total WSOA mass (Fig.9 b). The average concentration of water-soluble organic nitrogen (WSON) over the sampling period was 1.~~5~~16 μg N m^{-3} (~~114~~83.0 nmol N m^{-3}), which is in fact much lower than those measured in Beijing (226 nmol N m^{-3}) ~~(Duan et al., 2009)~~(Duan et al., 2009), Qingdao (129~~- -~~ 199 nmol N m^{-3}) ~~(Shi et al., 2010)~~(Shi et al., 2010), Xi,an (300 nmol N m^{-3}) ~~(Ho et al., 2015)~~(Ho et al., 2015). The concentration of water-soluble inorganic

nitrogen (WSIN, N from ammonium, nitrate and nitrite) was ~~8.7~~14.0 μg N m^{-3} base on Table ~~2~~3, and thus the WSON content corresponds to ~~14.9~~7.7% of water-soluble nitrogen (WSN = WSON +WSIN). This values is also much lower than those in Beijing (~30%) ~~(Duan et al., 2009)~~(Duan et al., 2009), Qingdao (19-~~ ~~~~22.6%), and Xi,an (22-~~ ~~~~68%) (Ho et al., 2015).

域代码已更改

Nevertheless, the level of ON measured here are a few times higher than those observed in other locations from AMS measurements (typically 1-~~ ~~3%) ~~(Xu et al., 2014)~~(Xu et al., 2014), likely due to the following reasons: First, previous studies were online measurements on non-refractory submicron aerosols, while it is likely that the supermicron fine particles (1-2.5 μm) contain significant nitrogen-containing species, as observed before for marine aerosols ~~(Violaki and Mihalopoulos, 2010)~~(Violaki and Mihalopoulos, 2010). Secondly, we measured only the water-soluble fraction of OA, which may concentrate more nitrogen-containing species (partially from aqueous-phase processing). Thirdly, a recent study reveals that fossil fuel combustion-related emission can be a dominant source of ammonia in urban area~~,~~ (Pan et al., 2016), it thus can act as a significant contributor to amines as amines are often co-emitted with ammonia ~~(Ge et al., 2011b)~~(Ge et al., 2011b); these amines can be neutralized by inorganic or organic acids and since aminium salts are highly hygroscopic ~~(Ge et al., 2011a)~~(Ge et al., 2011a), they might be enriched in the WSOA, and generated significant $C_xH_yN_p^+$ ions. Nevertheless, more AMS analyses on the water-extracted $PM_{2.5}$ samples collected from other locations should be conducted to further verify the abundance of ON species in the AMS mass spectra of WSOA.

Overall, the average elemental ratios of the WSOA are 0.~~36~~54 for O/C, 1.~~54~~69 for H/C, 0.11 for N/C and 1.~~74~~99 for OM/OC (Fig. 9a). WSOA is on average comprised of ~~61.4~~50.2% C, 7~~.2~~.1 % H, ~~22.9~~36.1% O, ~~8~~6.4% N and a negligible fraction (0.2%) of S (Fig. 9b). ~~Except for the enrichment of ON, other results are similar with other online AMS measurement results, such as in Fresno (Ge et al., 2012a).~~

3.6.2 WSOA sources from PMF analysis

The PMF analysis of the WSOA HRMS matrix identified four OA factors, including two primary OA (POA) factors, named as ~~the~~ nitrogen-enriched hydrocarbon-like OA (NHOA), and ~~cooking-relevant~~local primary OA (~~COA~~LOA), and two secondary OA factors which are a less oxidized oxygenated OA (LO-OOA) and a more oxidized oxygenated OA (MO-OOA), as shown in Fig. 10.

The NHOA factor had a low O/C ratio (0.~~14~~19), and was abundant in $C_xH_y^+$ ions (33.8%) and the NHOA time series also varied closely with those ions, ~~showing~~representing its ~~common feature~~features as traffic-related OA. In particular, the factor was rich in $C_xH_yN_p^+$ ions (43.1%), as a result, it shows a much higher N/C ratio (0.26, Fig. 10a) than other factors, and correlated well with CHN^+ (~~r^2=~~r = 0.~~82~~91), CH_4N^+ (~~r^2=~~r = 0.~~90), and~~95), CH_2N^+ (~~r^2=~~r = 0.~~70~~85), and $C_2H_4N^+$ (~~r^2=~~r = 0.~~76~~87) (Fig. 10b). The N-containing ions in the NHOA MS were dominated by the reduced ions ($C_xH_yN^+$) rather than oxidized ones ($C_xH_yO_zN^+$), suggesting that amino compounds were likely the major ON species, and was in consistent with our hypothesis aforementioned in Section 3.6.1 that they were mainly from ~~traffic~~fossil fuel combustion emissions. Nevertheless, future studies should be conducted to investigate in details the contribution of ~~traffic source~~fossil fuel combustion to the atmospheric ON species.

~~The COA~~Another primary OA factor was defined as a local primary OA (LOA) contains contributions from mixed anthropogenic emissions, such as cooking, coal combustion, etc. LOA had a low O/C ratio of 0.~~14~~19 and also contained mainly reduced $C_xH_y^+$ ions (60.8%) as well, ~~representing~~verifying its primary origin. ~~Its~~Note its mass ~~spectrum~~profile is characterized by peaks at *m/z* 55 (significant $C_3H_3O^+$) and *m/z* 57 (significant $C_3H_5O^+$). The abundance of $C_3H_3O^+$ at *m/z* 55 and $C_3H_5O^+$ at *m/z* 57 is a spectral feature of cooking OA, and the overall COA MS and O/C ratios are also similar to the COA factors reported in other studies, such as in Beijing~~ (Sun et al., 2016). The COA time series also correlated well with other cooking related marker ions, such as $C_5H_8O^+$ (r^2=0.58), $C_6H_{10}O^+$ (r^2 = 0.54), $C_7H_{12}O^+$ (r^2=0.45), consistent with the observations from many previous studies (e.g., Sun et al., 2011b;Ge et al., 2012a). All these results indicate its feature as cooking-related OA. However, the ratio of COA~~. The

LOA time series also correlated well with other cooking-related marker ions, such as $C_5H_8O^+$ (r = 0.76), $C_6H_{10}O^+$ (r = 0.74), $C_7H_{12}O^+$ (r = 0.67), consistent with the cooking OA from many previous studies (e.g., Sun et al., 2011b;Ge et al., 2012a). All these results indicate the LOA may have significant contributions from cooking activities. However, the ratio of LOA/$C_6H_{10}O^+$ (622.0) in this study was much higher than that obtained in winter in Fresno and New York City (~180), ~~likely due to we only detected the water soluble fraction of COA~~and also its mass fraction to the total OA was a few times higher than previous results, suggesting that it contains species from other primary sources rather than only cooking emissions.

The LO-OOA MS profile exhibited characteristics of oxidized OA with enhanced signals at *m/z* 29 (CHO^+), *m/z* 43 (mainly $C_2H_3O^+$) and other oxygenated ions. Tight correlations between time series of LO-OOA and CHO^+ (~~r^2=~~r = 0.~~84~~92), and $C_2H_3O^+$ (~~r^2=~~r = 0.~~54~~73) were also observed. Moreover, we also noticed relatively high signals of the BBOA tracer ions $C_2H_4O_2^+$ and $C_3H_5O_2^+$ in the LO-OOA MS, and found good correlations between LO-OOA and BBOA tracers (~~r^2=~~r = 0.~~76~~87 with $C_2H_4O_2^+$, and ~~r^2=~~r = 0.~~86~~93 with $C_3H_5O_2^+$), indicating possible influence from biomass burning~~ on the LO-OOA.~~. Thus, we compared mass fraction of LO-OOA to total OA in different seasons assuming that LO-OOA contributions would increase in straw-burning seasons given that it could be influenced by BBOA. Figure S6 showed the mass fraction of four factors during straw-burning seasons (spring, summer) and non-straw burning seasons (fall, winter). No obvious difference for LO-OOA fraction was found~~, thus this factor is in fact not heavily influenced by BBOA.~~. Furthermore, the O/C and OM/OC ratios were 0.53 and 1.95, corresponding to 0.34 and 1.~~70~~62 if calculated by using method of Aiken et al. (2008), well within the O/C range of less-oxidized OA factors identified in other studies ~~(Jimenez et al., 2009)~~(Jimenez et al., 2009), but beyond the O/C range of typical BBOA (0.18~~- -~~ 0.26) ~~(He et al., 2010)~~(He et al., 2010)~~. On the other hand, the~~.

The MO-OOA factor had prominent peaks at *m/z* 28 (mainly CO^+) and *m/z* 44 (mainly CO_2^+), and was dominated by $C_xH_yO_1^+$ (36.6%) and $C_xH_yO_2^+$ ions (29.0%) (Fig. 10a). As a result, MO-OOA had a very high O/C ratio of 1.~~04~~20, showing that it is

heavily aged and processed OA component. Correspondingly, its time series correlated well with the secondary OA tracer ions, such as CO_2^+ (~~r^2~~=r = 0.~~87) (Fig. 10b~~93), $C_2H_4O^+$ (~~r^2~~=r = 0.~~45~~67) and $C_2H_3O^+$ (~~r^2~~=r = 0.~~53~~73) (Fig. 10b), etc.

The *f*44 (mass fraction of *m/z* 44 to the total OA) ~~versus~~*vs.* *f*43 (mass fraction of *m/z* 43 to the total OA, defined by ~~Ng et al. (2010)~~Ng et al. (2010)), can be used to investigate the degree of oxygenation of the identified factors. As presented in Fig. 11a, apart from NHOA, other three factors (~~COA~~LOA, LO-OOA and MO-OOA) all fall within the triangular region. MO-OOA located at the upper position with a higher *f*44 of 0.28, while LO-OOA located at the lower position of plot as it had a high fraction of *f*43 (0.09). This distribution of the four factors is also consistent with other studies.

The mass contributions of the four factors to total WSOA over the whole year are 23.9% for NHOA, 31.2% for ~~COA~~LOA, 15.3% for LO-OOA and 29.7% for MO-OOA (Fig. 11b). POA (= NHOA~~+COA~~ + LOA) overweighed SOA (= LO-OOA~~+~~ + MO-OOA) mass, showing the dominant role of local anthropogenic emissions to the aerosol pollution in Changzhou, similar to that observed in Nanjing ~~(Wang et al., 2016b)~~(Wang et al., 2016b). However, during spring and winter, SOA contributions dominate over POA, indicating significant SOA formation in particular the MO-OOA during cold seasons, which is in agreement with the OC/EC results. —

3.7 Back trajectory clustering analysis

The Hybrid Single-particle Lagrangian Intergrated trajectory (HYSPLIT) model (Draxler et al., 2012) was used to investigate the origins of air masses based on the meteorological data available at the National Oceanic and Atmospheric Administration (NOAA) Global Data Assimilation System (GDAS). The 72h back trajectories of air parcels at 100 m above ground level in Changzhou were calculated at 8:00 local time (LT) throughout the campaign, and the results were presented in Fig. 12. The 4-, 5-, 4-, and 4-cluster solutions were adopted for spring, summer, fall and winter, respectively. During summer, air masses from southeast, east and west directions, passing over Shanghai and Anhui province, dominated the trajectories (75%) air masses. West and northwest air parcels dominated during winter, which may intercept air pollutants from

Hebei and Anhui province. Considering the relatively short sampling days in each season, a more detailed discussion that is useful to distinguish contributions of local, regional and long-range transport to the air pollution, will be the subject of our future work.

带格式的: 缩进: 首行缩进: 0 字符

4. Conclusions

We presented here the comprehensive characterization results on the $PM_{2.5}$ samples collected across one year in Changzhou City, located in the YRD region of China. The species we quantified including WSIIs, trace metals, EC, WSOA, WIOA and also PAHs, can reproduce on average ~80% mass of the $PM_{2.5}$ (108.3 μg m^{-3}). WSIIs were the major component, accounting for 52.1% $PM_{2.5}$ mass, and NO_3^-, SO_4^{2-}, NH_4^+ were three most abundant ions. The organic matter (the sum of WSOA and WIOA) occupied ~20~~20~~21.5% $PM_{2.5}$ mass, and EC accounted for ~5% $PM_{2.5}$ mass. Trace metal elements accounted for ~~6~~5% and ~2.7% $PM_{2.5}$ mass during winter and spring. Total PAHs concentrations were found to be at a relatively high concentration of 140.25 ng m^{-3} in winter, above three times the average mass loading of 41.42 ng m^{-3} in spring, both with InP, BghiP and Chr as the three most abundant PAHs. Average mass ratio of NO_3^-/SO_4^{2-} was 1.21, suggesting a significant role of traffic emissions, which is in consistent with the source analyses results based on the diagnostic ratios of the selected PAHs (BaP/BghiP, Flua/(Flua+Pyr) and BaP/(BaP+Chr)). In addition, a high Cl^-/Na^+ ratio and the diagnostic ratio of Phe/(Ant+Phe) indicated also the contribution from coal combustion, in particular during winter.

In order to obtain further information regarding particle source, we analyzed the WSOA using SP-AMS and conducted PMF analyses on the HRMS of WSOA. Four OA factors including NHOA, ~~COA~~LOA, LO-OOA and MO-OOA were identified. The mean mass contribution of POA ~~(=NHOA+COA)~~ was larger than that of SOA ~~(=LO-OOA+MO-OOA),~~ revealing that local anthropogenic activities are the major drivers of PM pollution in Changzhou. Nevertheless, during cold seasons, SOA mass contribution increased, indicating significant role of secondarily formed species as well,

thus reduction of air pollution in Changzhou should be paid on the strict emission control of both primary particles and the gaseous secondary aerosol precursors. One interesting finding in this work is the enrichment of organic nitrogen species in WSOA, and source analysis indicates that traffic emissions can be a significant contributor to these species, which warrants more detailed investigations in the future. Also, more offline samples should be collected to achieve a more robust PMF analyses. Simultaneous online AMS measurement on the fine particles and measurements of gaseous species (SO_2, NO_2, O_3, CO and some volatile organic compounds) are also essential to better understand the aerosol characteristics, and to implement proper measures to abate the air pollution in this region.

Acknowledgements

This work was supported the Natural Science Foundation of China (Grant Nos. (21407079 and 91544220), the Jiangsu National Science Foundation (BK20150042), the Specially-Appointed Professors Foundation and Jiangsu Innovation and Entrepreneurship Program (for X.G.), and the Major Research Development Program of Jiangsu Province (BE2016657 and BY2016030-15~~), the open fund by Jiangsu Key Laboratory of Atmospheric Environment Monitoring and Pollution Control (KHK1409),.~~). We would also like to acknowledge Mr. Gang Li from Chinese academy of Science for providing us the OC/EC measurements.

References:

Aiken, A. C., Decarlo, P. F., Kroll, J. H., Worsnop, D. R., Huffman, J. A., Docherty, K. S., Ulbrich, I. M., Mohr, C., Kimmel, J. R., Sueper, D., Sun, Y., Zhang, Q., Trimborn, A., Northway, M., Ziemann, P. J., Canagaratna, M. R., Onasch, T. B., Alfarra, M. R., Prevot, A. S. H., Dommen, J., Duplissy, J., Metzger, A., Baltensperger, U., and Jimenez, J. L.: O/C and OM/OC ratios of primary, secondary, and ambient organic aerosols with high-resolution time-of-flight aerosol mass spectrometry, Environ. Sci. Technol., 42, 4478-4485, doi: 10.1021/Es703009q, 2008.

Anderson, J. O., Thundiyil, J. G., and Stolbach, A.: Clearing the air: A review of the effects of particulate matter air pollution on human health, J. Med. Toxicol., 8, 166-175, doi: 10.1007/s13181-011-0203-1, 2012.

790 Arimoto, R., Duce, R. A., Savoie, D. L., Prospero, J. M., Talbot, R., Cullen, J. D., Tomza, U.,
791 Lewis, N. F., and Ray, B. J.: Relationships among aerosol constituents from Asia and the North
792 Pacific during PEM-West A, J. Geophys. Res. -Atmos., 101, 2011-2023, doi:
793 10.1029/95JD01071, 1996.

794 Bozzetti, C., Sosedova, Y., Xiao, M., Daellenbach, K. R., Ulevicius, V., Dudoitis, V., Mordas,
795 G., Byčenkienė, S., Plauškaitė, K., Vlachou, A., Golly, B., Chazeau, B., Besombes, J. L.,
796 Baltensperger, U., Jaffrezo, J. L., Slowik, J. G., El Haddad, I., and Prévôt, A. S. H.: Argon
797 offline-AMS source apportionment of organic aerosol over yearly cycles for an urban, rural, and
798 marine site in northern Europe, Atmos. Chem. Phys., 17, 117-141, doi:
799 10.5194/acp-17-117-2017, 2017.

800 Canagaratna, M. R., Jayne, J. T., Jimenez, J. L., Allan, J. D., Alfarra, M. R., Zhang, Q., Onasch,
801 T. B., Drewnick, F., Coe, H., Middlebrook, A., Delia, A., Williams, L. R., Trimborn, A. M.,
802 Northway, M. J., DeCarlo, P. F., Kolb, C. E., Davidovits, P., and Worsnop, D. R.: Chemical and
803 microphysical characterization of ambient aerosols with the aerodyne aerosol mass spectrometer,
804 Mass Spectrom Rev, 26, 185-222, doi: 10.1002/Mas.20115, 2007.

805 Canagaratna, M. R., Jimenez, J. L., Kroll, J. H., Chen, Q., Kessler, S. H., Massoli, P.,
806 Hildebrandt Ruiz, L., Fortner, E., Williams, L. R., Wilson, K. R., Surratt, J. D., Donahue, N. M.,
807 Jayne, J. T., and Worsnop, D. R.: Elemental ratio measurements of organic compounds using
808 aerosol mass spectrometry: characterization, improved calibration, and implications, Atmos.
809 Chem. Phys., 15, 253-272, doi: 10.5194/acp-15-253-2015, 2015.

810 Cao, J. J., Xu, H. M., Xu, Q., Chen, B. H., and Kan, H. D.: Fine particulate matter constituents
811 and cardiopulmonary mortality in a heavily polluted Chinese city, Environ. Health Persp., 120,
812 373-378, doi: 10.1289/ehp.1103671, 2012.

813 Cheng, Y., He, K. B., Du, Z. Y., Zheng, M., Duan, F. K., and Ma, Y. L.: Humidity plays an
814 important role in the PM(2).(5) pollution in Beijing, Environ. Pollut., 197, 68-75, doi:
815 10.1016/j.envpol.2014.11.028, 2015.

816 Chow, J. C., Watson, J. G., Chen, L. W. A., Arnott, W. P., Moosmüller, H., and Fung, K.:
817 Equivalence of elemental carbon by thermal/optical reflectance and transmittance with different
818 temperature protocols, Environ. Sci. Technol. , 38, 4414-4422, doi: 10.1021/es034936u, 2004.

819 Chow, J. C., Watson, J. G., Louie, P. K., Chen, L. W., and Sin, D.: Comparison of PM2.5 carbon
820 measurement methods in Hong Kong, China, Environ. Pollut., 137, 334-344, doi:
821 10.1016/j.envpol.2005.01.006, 2005.

822 Daellenbach, K. R., Bozzetti, C., Křepelová, A., Canonaco, F., Wolf, R., Zotter, P., Fermo, P.,
823 Crippa, M., Slowik, J. G., Sosedova, Y., Zhang, Y., Huang, R. J., Poulain, L., Szidat, S.,
824 Baltensperger, U., El Haddad, I., and Prévôt, A. S. H.: Characterization and source
825 apportionment of organic aerosol using offline aerosol mass spectrometry, Atmos. Meas. Tech.,
826 9, 23-39, doi: 10.5194/amt-9-23-2016, 2016.

Ding, A. J., Fu, C. B., Yang, X. Q., Sun, J. N., Zheng, L. F., Xie, Y. N., Herrmann, E., Nie, W., Petaja, T., Kerminen, V. M., and Kulmala, M.: Ozone and fine particle in the western Yangtze River Delta: an overview of 1 yr data at the SORPES station, Atmos. Chem. Phys., 13, 5813-5830, doi: 10.5194/acp-13-5813-2013, 2013.

Draxler, R., Stunder, B., Rolph, G., Stein, A., and Taylor, A.: HYSPLIT4 user's guide, version 4, report, NOAA, Silver Spring, MD, doi, 2012.

Drewnick, F.: Speciation analysis in on-line aerosol mass spectrometry, Anal. Bioanal. Chem., 404, 2127-2131, doi: 10.1007/s00216-012-6295-x, 2012.

Duan, F., Liu, X., He, K., and Dong, S.: Measurements and characteristics of nitrogen-containing compounds in atmospheric particulate matter in Beijing, China, Bull. Environ. Contam. Toxicol., 82, 332-337, doi: 10.1007/s00128-008-9560-0, 2009.

Duan, J., Tan, J., Wang, S., Chai, F., He, K., and Hao, J.: Roadside, urban, and rural comparison of size distribution characteristics of PAHs and carbonaceous components of Beijing, China, J. Atmos. Chem., 69, 337-349, doi: 10.1007/s10874-012-9242-5, 2012.

Dzepina, K., Arey, J., Marr, L. C., Worsnop, D. R., Salcedo, D., Zhang, Q., Onasch, T. B., Molina, L. T., Molina, M. J., and Jimenez, J. L.: Detection of particle-phase polycyclic aromatic hydrocarbons in Mexico City using an aerosol mass spectrometer, Int. J. Mass Spectrom., 263, 152-170, doi: 10.1016/j.ijms.2007.01.010, 2007.

Fan, J., Yue, X., Jing, Y., Chen, Q., and Wang, S.: Online monitoring of water-soluble ionic composition of PM10 during early summer over Lanzhou City, J. Environ. Sci., 26, 353-361, doi: 10.1016/s1001-0742(13)60431-3, 2014.

Feng, J., Hu, J., Xu, B., Hu, X., Sun, P., Han, W., Gu, Z., Yu, X., and Wu, M.: Characteristics and seasonal variation of organic matter in PM2.5 at a regional background site of the Yangtze River Delta region, China, Atmos. Environ., 123, 288-297, doi: 10.1016/j.atmosenv.2015.08.019, 2015.

Feng, Y., Chen, Y., Guo, H., Zhi, G., Xiong, S., Li, J., Sheng, G., and Fu, J.: Characteristics of organic and elemental carbon in PM2.5 samples in Shanghai, China, Atmos. Res., 92, 434-442, doi: 10.1016/j.atmosres.2009.01.003, 2009.

Fu, H., Zhang, M., Li, W., Chen, J., Wang, L., Quan, X., and Wang, W.: Morphology, composition and mixing state of individual carbonaceous aerosol in urban Shanghai, Atmos. Chem. Phys., 12, 693-707, doi: 10.5194/acp-12-693-2012, 2012.

Ge, X., Wexler, A. S., and Clegg, S. L.: Atmospheric amines - Part II. Thermodynamic properties and gas/particle partitioning, Atmos. Environ., 45, 561-577, doi: DOI 10.1016/j.atmosenv.2010.10.013, 2011a.

Ge, X., Wexler, A. S., and Clegg, S. L.: Atmospheric amines - Part I. A review, Atmos. Environ., 45, 524-546, doi: DOI 10.1016/j.atmosenv.2010.10.012, 2011b.

Ge, X., Setyan, A., Sun, Y., and Zhang, Q.: Primary and secondary organic aerosols in Fresno, California during wintertime: Results from high resolution aerosol mass spectrometry, J. Geophys. Res. -Atmos., 117, D19301, doi: 10.1029/2012jd018026, 2012a.

Ge, X., Zhang, Q., Sun, Y., Ruehl, C. R., and Setyan, A.: Effect of aqueous-phase processing on aerosol chemistry and size distributions in Fresno, California, during wintertime, Environ. Chem., 9, 221-235, doi: 10.1071/EN11168, 2012b.

Ge, X., Shaw, S. L., and Zhang, Q.: Toward understanding amines and their degradation products from postcombustion CO2 capture processes with aerosol mass spectrometry, Environ. Sci. Technol., 48, 5066-5075, doi: 10.1021/es4056966, 2014.

Ge, X., Wang, J., Zhang, Z., Wang, X., and Chen, M.: Thermodynamic modeling of electrolyte solutions by a hybrid ion-interaction and solvation (HIS) model, Calphad, 48, 79-88, doi: 10.1016/j.calphad.2014.11.001, 2015.

Gu, J., Bai, Z., Liu, A., Wu, L., Xie, Y., Li, W., Dong, H., and Zhang, X.: Characterization of atmospheric organic carbon and element carbon of PM2.5 and PM10 at Tianjin, China, Aerosol Air Qual. Res., 10, 167-176, doi: 10.4209/aaqr.2009.12.0080, 2010.

Gu, J., Du, S., Han, D., Hou, L., Yi, J., Xu, J., Liu, G., Han, B., Yang, G., and Bai, Z.-P.: Major chemical compositions, possible sources, and mass closure analysis of PM2.5 in Jinan, China, Air Qual. Atmos. Health, 7, 251-262, doi: 10.1007/s11869-013-0232-9, 2014.

He, J., Fan, S., Meng, Q., Sun, Y., Zhang, J., and Zu, F.: Polycyclic aromatic hydrocarbons (PAHs) associated with fine particulate matters in Nanjing, China: Distributions, sources and meteorological influences, Atmos. Environ., 89, 207-215, doi: 10.1016/j.atmosenv.2014.02.042, 2014.

He, L. Y., Lin, Y., Huang, X. F., Guo, S., Xue, L., Su, Q., Hu, M., Luan, S. J., and Zhang, Y. H.: Characterization of high-resolution aerosol mass spectra of primary organic aerosol emissions from Chinese cooking and biomass burning, Atmos. Chem. Phys., 10, 11535-11543, doi: 10.5194/acp-10-11535-2010, 2010.

Heal, M. R., Kumar, P., and Harrison, R. M.: Particles, air quality, policy and health, Chem. Soc. Rev., doi, 2012.

Ho, K. F., Ho, S. S. H., Huang, R.-J., Liu, S. X., Cao, J.-J., Zhang, T., Chuang, H.-C., Chan, C. S., Hu, D., and Tian, L.: Characteristics of water-soluble organic nitrogen in fine particulate matter in the continental area of China, Atmos. Environ., 106, 252-261, doi: 10.1016/j.atmosenv.2015.02.010, 2015.

Hu, J., Ying, Q., Wang, Y., and Zhang, H.: Characterizing multi-pollutant air pollution in China: Comparison of three air quality indices, Environ. Int., 84, 17-25, doi: 10.1016/j.envint.2015.06.014, 2015.

Hu, W., Hu, M., Hu, W., Jimenez, J. L., Yuan, B., Chen, W., Wang, M., Wu, Y., Chen, C.,

Wang, Z., Peng, J., Zeng, L., and Shao, M.: Chemical composition, sources, and aging process of submicron aerosols in Beijing: Contrast between summer and winter, J. Geophys. Res. -Atmos., 121, 2015JD024020, doi: 10.1002/2015JD024020, 2016.

Hu, X., Zhang, Y., Ding, Z., Wang, T., Lian, H., Sun, Y., and Wu, J.: Bioaccessibility and health risk of arsenic and heavy metals (Cd, Co, Cr, Cu, Ni, Pb, Zn and Mn) in TSP and PM2.5 in Nanjing, China, Atmos. Environ., 57, 146-152, doi: 10.1016/j.atmosenv.2012.04.056, 2012.

Huang, R., Zhang, Y., Bozzetti, C., Ho, K., Cao, J., Han, Y., Daellenbach, K. R., Slowik, J. G., Platt, S. M., Canonaco, F., Zotter, P., Wolf, R., Pieber, S. M., Bruns, E. A., Crippa, M., Ciarelli, G., Piazzalunga, A., Schwikowski, M., Abbaszade, G., Schnelle-Kreis, J., Zimmermann, R., An, Z., Szidat, S., Baltensperger, U., Haddad, I. E., and Prevot, A. S. H.: High secondary aerosol contribution to particulate pollution during haze events in China, Nature, 514, 218-222, doi: 10.1038/nature13774, 2014.

Huang, T., Chen, J., Zhao, W., Cheng, J., and Cheng, S.: Seasonal variations and correlation analysis of water-soluble inorganic ions in PM2.5 in Wuhan, 2013, Atmosphere, 7, 49, doi: 10.3390/atmos7040049, 2016.

Huang, X. F., He, L. Y., Hu, M., Canagaratna, M. R., Sun, Y., Zhang, Q., Zhu, T., Xue, L., Zeng, L. W., Liu, X. G., Zhang, Y. H., Jayne, J. T., Ng, N. L., and Worsnop, D. R.: Highly time-resolved chemical characterization of atmospheric submicron particles during 2008 Beijing Olympic Games using an Aerodyne High-Resolution Aerosol Mass Spectrometer, Atmos. Chem. Phys., 10, 8933-8945, doi: 10.5194/acp-10-8933-2010, 2010.

Jimenez, J. L., Canagaratna, M. R., Donahue, N. M., Prevot, A. S. H., Zhang, Q., Kroll, J. H., DeCarlo, P. F., Allan, J. D., Coe, H., Ng, N. L., Aiken, A. C., Docherty, K. S., Ulbrich, I. M., Grieshop, A. P., Robinson, A. L., Duplissy, J., Smith, J. D., Wilson, K. R., Lanz, V. A., Hueglin, C., Sun, Y. L., Tian, J., Laaksonen, A., Raatikainen, T., Rautiainen, J., Vaattovaara, P., Ehn, M., Kulmala, M., Tomlinson, J. M., Collins, D. R., Cubison, M. J., Dunlea, E. J., Huffman, J. A., Onasch, T. B., Alfarra, M. R., Williams, P. I., Bower, K., Kondo, Y., Schneider, J., Drewnick, F., Borrmann, S., Weimer, S., Demerjian, K., Salcedo, D., Cottrell, L., Griffin, R., Takami, A., Miyoshi, T., Hatakeyama, S., Shimono, A., Sun, J. Y., Zhang, Y. M., Dzepina, K., Kimmel, J. R., Sueper, D., Jayne, J. T., Herndon, S. C., Trimborn, A. M., Williams, L. R., Wood, E. C., Middlebrook, A. M., Kolb, C. E., Baltensperger, U., and Worsnop, D. R.: Evolution of organic aerosols in the atmosphere, Science, 326, 1525-1529, doi: 10.1126/science.1180353, 2009.

Khalili, N. R., Scheff, P. A., and Holsen, T. M.: PAH source fingerprints for coke ovens, diesel and, gasoline engines, highway tunnels, and wood combustion emissions, Atmos. Environ., 29, 533-542, doi: 10.1016/1352-2310(94)00275-P, 1995.

Kong, S., Ding, X., Bai, Z., Han, B., Chen, L., Shi, J., and Li, Z.: A seasonal study of polycyclic aromatic hydrocarbons in PM(2.5) and PM(2.5-10) in five typical cities of Liaoning Province, China, J. Hazard. Mater., 183, 70-80, doi: 10.1016/j.jhazmat.2010.06.107, 2010.

Kong, S., Li, X., Li, L., Yin, Y., Chen, K., Yuan, L., Zhang, Y., Shan, Y., and Ji, Y.: Variation

of polycyclic aromatic hydrocarbons in atmospheric PM2.5 during winter haze period around 2014 Chinese Spring Festival at Nanjing: Insights of source changes, air mass direction and firework particle injection, Sci. Total Environ., 520, 59-72, doi: 10.1016/j.scitotenv.2015.03.001, 2015.

Kulmala, M., Lappalainen, H. K., Petäjä, T., Kurten, T., Kerminen, V. M., Viisanen, Y., Hari, P., Sorvari, S., Bäck, J., Bondur, V., Kasimov, N., Kotlyakov, V., Matvienko, G., Baklanov, A., Guo, H. D., Ding, A., Hansson, H. C., and Zilitinkevich, S.: Introduction: The Pan-Eurasian Experiment (PEEX) – multidisciplinary, multiscale and multicomponent research and capacity-building initiative, Atmos. Chem. Phys., 15, 13085-13096, doi: 10.5194/acp-15-13085-2015, 2015.

Lee, A. K. Y., Willis, M. D., Healy, R. M., Onasch, T. B., and Abbatt, J. P. D.: Mixing state of carbonaceous aerosol in an urban environment: single particle characterization using the soot particle aerosol mass spectrometer (SP-AMS), Atmos. Chem. Phys., 15, 1823-1841, doi: 10.5194/acp-15-1823-2015, 2015.

Li, B., Zhang, J., Zhao, Y., Yuan, S., Zhao, Q., Shen, G., and Wu, H.: Seasonal variation of urban carbonaceous aerosols in a typical city Nanjing in Yangtze River Delta, China, Atmos. Environ., 106, 223-231, doi: 10.1016/j.atmosenv.2015.01.064, 2015.

Liu, G., Li, J., Wu, D., and Xu, H.: Chemical composition and source apportionment of the ambient PM2.5 in Hangzhou, China, Particuology, 18, 135-143, doi: 10.1016/j.partic.2014.03.011, 2015.

Meng, C. C., Wang, L. T., Zhang, F. F., Wei, Z., Ma, S. M., Ma, X., and Yang, J.: Characteristics of concentrations and water-soluble inorganic ions in PM2.5 in Handan City, Hebei province, China, Atmos. Res., 171, 133-146, doi: 10.1016/j.atmosres.2015.12.013, 2016.

Mihara, T., and Mochida, M.: Characterization of Solvent-Extractable Organics in Urban Aerosols Based on Mass Spectrum Analysis and Hygroscopic Growth Measurement, Environ. Sci. Technol., 45, 9168-9174, doi: 10.1021/es201271w, 2011.

Mirante, F., Salvador, P., Pio, C., Alves, C., Artiñano, B., Caseiro, A., and Revuelta, M. A.: Size fractionated aerosol composition at roadside and background environments in the Madrid urban atmosphere, Atmos. Res., 138, 278-292, doi: 10.1016/j.atmosres.2013.11.024, 2014.

Ng, N. L., Canagaratna, M. R., Zhang, Q., Jimenez, J. L., Tian, J., Ulbrich, I. M., Kroll, J. H., Docherty, K. S., Chhabra, P. S., Bahreini, R., Murphy, S. M., Seinfeld, J. H., Hildebrandt, L., Donahue, N. M., DeCarlo, P. F., Lanz, V. A., Prévôt, A. S. H., Dinar, E., Rudich, Y., and Worsnop, D. R.: Organic aerosol components observed in Northern Hemispheric datasets from Aerosol Mass Spectrometry, Atmos. Chem. Phys., 10, 4625-4641, doi: 10.5194/acp-10-4625-2010, 2010.

Ng, N. L., Canagaratna, M. R., Jimenez, J. L., Zhang, Q., Ulbrich, I. M., and Worsnop, D. R.: Real-time methods for estimating organic component mass concentrations from aerosol mass

spectrometer data, Environ. Sci. Technol., 45, 910-916, doi: Doi 10.1021/Es102951k, 2011.

Onasch, T. B., Trimborn, A., Fortner, E. C., Jayne, J. T., Kok, G. L., Williams, L. R., Davidovits, P., and Worsnop, D. R.: Soot particle aerosol mass spectrometer: Development, validation, and initial application, Aerosol Sci. Tech., 46, 804-817, doi: 10.1080/02786826.2012.663948, 2012.

Pan, Y., Tian, S., Liu, D., Fang, Y., Zhu, X., Zhang, Q., Zheng, B., Michalski, G., and Wang, Y.: Fossil Fuel Combustion-Related Emissions Dominate Atmospheric Ammonia Sources during Severe Haze Episodes: Evidence from 15N-Stable Isotope in Size-Resolved Aerosol Ammonium, Environ. Sci. Technol., 50, 8049-8056, doi: 10.1021/acs.est.6b00634, 2016.

Qi, L., Chen, M., Ge, X., Zhang, Y., and Guo, B.: Seasonal variations and sources of 17 aerosol metal elements in suburban Nanjing, China, Atmosphere, 7, 153, doi, 2016a.

Qi, L., Zhang, Y., Ma, Y., Chen, M., Ge, X., Ma, Y., Zheng, J., Wang, Z., and Li, S.: Source identification of trace elements in the atmosphere during the second Asian Youth Games in Nanjing, China: Influence of control measures on air quality, Atmos. Pollut. Res., 7, 547-556, doi: 10.1016/j.apr.2016.01.003, ~~2016~~2016b.

Qiao, T., Zhao, M., Xiu, G., and Yu, J.: Seasonal variations of water soluble composition (WSOC, Hulis and WSIIs) in PM1 and its implications on haze pollution in urban Shanghai, China, Atmos. Environ., 123, 306-314, doi: 10.1016/j.atmosenv.2015.03.010, 2015.

Saldarriaga-Noreña, H., López-Márquez, R., Murillo-Tovar, M., Hernández-Mena, L., Ospina-Noreña, E., Sánchez-Salinas, E., Waliszewski, S., and Montiel-Palma, S.: Analysis of PAHs associated with particulate matter PM2.5 in two places at the city of Cuernavaca, Morelos, México, Atmosphere, 6, 1259-1270, doi: 10.3390/atmos6091259, 2015.

Shen, G. F., Yuan, S. Y., Xie, Y. N., Xia, S. J., Li, L., Yao, Y. K., Qiao, Y. Z., Zhang, J., Zhao, Q. Y., Ding, A. J., Li, B., and Wu, H. S.: Ambient levels and temporal variations of PM2.5 and PM10 at a residential site in the mega-city, Nanjing, in the western Yangtze River Delta, China, J. Environ. Sci. Health A: Tox. Hazard. Subst. Environ..Eng., 49, 171-178, doi: 10.1080/10934529.2013.838851, 2014.

Shi, J., Gao, H., Qi, J., Zhang, J., and Yao, X.: Sources, compositions, and distributions of water-soluble organic nitrogen in aerosols over the China Sea, J. Geophys. Res. -Atmos., 115, doi: 10.1029/2009jd013238, 2010.

Sun, Y., Zhang, Q., Zheng, M., Ding, X., Edgerton, E. S., and Wang, X.: Characterization and source apportionment of water-soluble organic matter in atmospheric fine particles (PM2.5) with high-resolution aerosol mass spectrometry and GC-MS, Environ. Sci. Technol., 45, 4854-4861, doi: 10.1021/es200162h, 2011a.

Sun, Y., Jiang, Q., Wang, Z., Fu, P., Li, J., Yang, T., and Yin, Y.: Investigation of the sources and evolution processes of severe haze pollution in Beijing in January 2013, J. Geophys. Res. -Atmos., 119, 4380-4398, doi: 10.1002/2014jd021641, 2014.

Sun, Y., Du, W., Fu, P., Wang, Q., Li, J., Ge, X., Zhang, Q., Zhu, C., Ren, L., Xu, W., Zhao, J., Han, T., Worsnop, D. R., and Wang, Z.: Primary and secondary aerosols in Beijing in winter: sources, variations and processes, Atmos. Chem. Phys., 16, 8309-8329, doi: 10.5194/acp-16-8309-2016, 2016.

Sun, Y. L., Zhang, Q., Schwab, J. J., Demerjian, K. L., Chen, W. N., Bae, M. S., Hung, H. M., Hogrefe, O., Frank, B., Rattigan, O. V., and Lin, Y. C.: Characterization of the sources and processes of organic and inorganic aerosols in New York city with a high-resolution time-of-flight aerosol mass apectrometer, Atmos. Chem. Phys., 11, 1581-1602, doi: 10.5194/acp-11-1581-2011, 2011b.

Szabó, J., Nagy, A. S., and Erdős, J.: Ambient concentrations of PM10, PM10-bound polycyclic aromatic hydrocarbons and heavy metals in an urban site of Győr, Hungary, Air Qual. Atmos. Health, 8, 229-241, doi: 10.1007/s11869-015-0318-7, 2015.

Ulbrich, I. M., Canagaratna, M. R., Zhang, Q., Worsnop, D. R., and Jimenez, J. L.: Interpretation of organic components from Positive Matrix Factorization of aerosol mass spectrometric data, Atmos. Chem. Phys., 9, 2891-2918, doi: 10.5194/acp-9-2891-2009, 2009.

Violaki, K., and Mihalopoulos, N.: Water-soluble organic nitrogen (WSON) in size-segregated atmospheric particles over the Eastern Mediterranean, Atmos. Environ., 44, 4339-4345 doi, 2010.

Wang, F., Lin, T., Feng, J., Fu, H., and Guo, Z.: Source apportionment of polycyclic aromatic hydrocarbons in PM2.5 using positive matrix factorization modeling in Shanghai, China, Environ. Sci. Process Impacts, 17, 197-205, doi: 10.1039/c4em00570h, 2015.

Wang, F., Guo, Z., Lin, T., and Rose, N. L.: Seasonal variation of carbonaceous pollutants in PM2.5 at an urban 'supersite' in Shanghai, China, Chemosphere, 146, 238-244, doi: 10.1016/j.chemosphere.2015.12.036, 2016a.

Wang, G., Kawamura, K., Lee, S., Ho, K., and Cao, J.: Molecular, seasonal, and spatial distributions of organic aerosols from fourteen Chinese cities, Environ. Sci. Technol., 40, 4619-4625, doi: 10.1021/es060291x, 2006a.

Wang, J., Geng, N. B., Xu, Y. F., Zhang, W. D., Tang, X. Y., and Zhang, R. Q.: PAHs in PM2.5 in Zhengzhou: concentration, carcinogenic risk analysis, and source apportionment, Environ. Monit. Assess., 186, 7461-7473, doi: 10.1007/s10661-014-3940-1, 2014.

Wang, J., Ge, X., Chen, Y., Shen, Y., Zhang, Q., Sun, Y., Xu, J., Ge, S., Yu, H., and Chen, M.: Highly time-resolved urban aerosol characteristics during springtime in Yangtze River Delta, China: insights from soot particle aerosol mass spectrometry, Atmos. Chem. Phys., 16, 9109-9127, doi: 10.5194/acp-16-9109-2016, 2016b.

Wang, J., Onasch, T. B., Ge, X., Collier, S., Zhang, Q., Sun, Y., Yu, H., Chen, M., Prévôt, A. S. H., and Worsnop, D. R.: Observation of fullerene foot in eastern China, Environ. Sci. Technol.

带格式的: 非上标/ 下标

Lett., 3, 121-126, doi: 10.1021/acs.estlett.6b00044, 2016c.

Wang, T., Jiang, F., Deng, J., Shen, Y., Fu, Q., Wang, Q., Fu, Y., Xu, J., and Zhang, D.: Urban air quality and regional haze weather forecast for Yangtze River Delta region, Atmos. Environ., 58, 70-83, doi: 10.1016/j.atmosenv.2012.01.014, 2012.

Wang, Y., Zhuang, G., Zhang, X., Huang, K., Xu, C., Tang, A., Chen, J., and An, Z.: The ion chemistry, seasonal cycle, and sources of PM2.5 and TSP aerosol in Shanghai, Atmos. Environ., 40, 2935-2952, doi: 10.1016/j.atmosenv.2005.12.051, 2006b.

Xu, J., Zhang, Q., Li, X., Ge, X., Xiao, C., Ren, J., and Qin, D.: Dissolved organic matter and inorganic Ions in a central Himalayan glacier—Insights into chemical composition and atmospheric sources, Environ. Sci. Technol., 47, 6181-6188, doi: 10.1021/es4009882, 2013.

Xu, J., Zhang, Q., Chen, M., Ge, X., Ren, J., and Qin, D.: Chemical composition, sources, and processes of urban aerosols during summertime in northwest China: insights from high-resolution aerosol mass spectrometry, Atmos. Chem. Phys., 14, 12593-12611, doi: 10.5194/acp-14-12593-2014, 2014.

Xu, J., Zhang, Q., Wang, Z., Yu, G., Ge, X., and Qin, X.: Chemical composition and size distribution of summertime PM2.5 at a high altitude remote location in the northeast of the Qinghai–Xizang (Tibet) Plateau: insights into aerosol sources and processing in free troposphere, Atmos. Chem. Phys., 15, 5069-5081, doi: 10.5194/acp-15-5069-2015, 2015.

Xu, L., Guo, H., Weber, R. J., and Ng, N. L.: Chemical Characterization of Water-Soluble Organic Aerosol in Contrasting Rural and Urban Environments in the Southeastern United States, Environ. Sci. Technol., 51, 78-88, doi: 10.1021/acs.est.6b05002, 2017.

Ye, X. N., Ma, Z., Hu, D. W., Yang, X., and Chen, J. M.: Size-resolved hygroscopicity of submicrometer urban aerosols in Shanghai during wintertime, Atmos. Res., 99, 353-364, doi: 10.1016/j.atmosres.2010.11.008, 2011.

~~Young, D. E., Kim, H., Parworth, C., Zhou, S., Zhang, X., Cappa, C. D., Seco, R., Kim, S., and Zhang, Q.: Influences of emission sources and meteorology on aerosol chemistry in a polluted urban environment: results from DISCOVER-AQ California, Atmos. Chem. Phys., 16, 5427-5451, doi: 10.5194/acp-16-5427-2016, 2016.~~

Zhang, Q., Jimenez, J. L., Canagaratna, M. R., Allan, J. D., Coe, H., Ulbrich, I., Alfarra, M. R., Takami, A., Middlebrook, A. M., Sun, Y. L., Dzepina, K., Dunlea, E., Docherty, K., DeCarlo, P. F., Salcedo, D., Onasch, T., Jayne, J. T., Miyoshi, T., Shimono, A., Hatakeyama, S., Takegawa, N., Kondo, Y., Schneider, J., Drewnick, F., Borrmann, S., Weimer, S., Demerjian, K., Williams, P., Bower, K., Bahreini, R., Cottrell, L., Griffin, R. J., Rautiainen, J., Sun, J. Y., Zhang, Y. M., and Worsnop, D. R.: Ubiquity and dominance of oxygenated species in organic aerosols in anthropogenically-influenced Northern Hemisphere midlatitudes, Geophys. Res. Lett., 34, n/a-n/a, doi: 10.1029/2007gl029979, ~~2007~~2007a.

带格式的: 非上标/ 下标

Zhang, Q., Jimenez, J. L., Worsnop, D. R., and Canagaratna, M.: A case study of urban particle acidity and its influence on secondary organic aerosol, Environ. Sci. Technol., 41, 3213-3219, doi: 10.1021/Es061812j, 2007b.

Zhang, Q., Jimenez, J. L., Canagaratna, M. R., Ulbrich, I. M., Ng, N. L., Worsnop, D. R., and Sun, Y.: Understanding atmospheric organic aerosols via factor analysis of aerosol mass spectrometry: a review, Anal. Bioanal. Chem., 401, 3045-3067, doi: 10.1007/s00216-011-5355-y, 2011.

Zhang, R., Jing, J., Tao, J., Hsu, S. C., Wang, G., Cao, J., Lee, C. S. L., Zhu, L., Chen, Z., Zhao, Y., and Shen, Z.: Chemical characterization and source apportionment of PM2.5 in Beijing: seasonal perspective, Atmos. Chem. Phys., 13, 7053-7074, doi: 10.5194/acp-13-7053-2013, 2013.

Zhang, Y. J., Tang, L., Yu, H., Wang, Z., Sun, Y., Qin, W., Chen, W., Chen, C., Ding, A., Wu, J., Ge, S., Chen, C., and Zhou, H.-c.: Chemical composition, sources and evolution processes of aerosol at an urban site in Yangtze River Delta, China during wintertime, Atmos. Environ., 123, 339-349, doi: 10.1016/j.atmosenv.2015.08.017, 2016.

Zhao, M., Huang, Z., Qiao, T., Zhang, Y., Xiu, G., and Yu, J.: Chemical characterization, the transport pathways and potential sources of PM2.5 in Shanghai: Seasonal variations, Atmos. Res., 158-159, 66-78, doi: 10.1016/j.atmosres.2015.02.003, 2015.

Zhou, J., Xing, Z., Deng, J., and Du, K.: Characterizing and sourcing ambient PM2.5 over key emission regions in China I: Water-soluble ions and carbonaceous fractions, Atmos. Environ., 135, 20-30, doi: 10.1016/j.atmosenv.2016.03.054, 2016.

带格式的: 非上标/ 下标

带格式的: 非上标/ 下标

带格式的: 非上标/ 下标

Table 1. Average meteorological parameters during four seasons

Parameters	Spring	Summer	Fall	Winter
RH (%)	57.3±11.4	61.1±11.8	65.5±10.9	62.3±10.6
T(^{o}C)	13.1±4.0	32.1±4.3	21.6±2.3	5.6±1.8
WS(m s^{-1})	1.1±0.4	1.6±0.6	0.9±0.4	0.89±0.3
WD[a]	SE	E,W,SE	E	W,NW,SE

[a] Refer to prevailing wind directions, E—East, SE—Southeast, W—West, NW-Northwest.

带格式的: 字体: 12 磅
带格式的: 字体: 12 磅
带格式的: 字体: 12 磅
带格式的: 字体: 12 磅
带格式的: 字体: 12 磅
带格式的: 缩进: 首行缩进: 0.5 字符
带格式的: 缩进: 首行缩进: 0 字符
带格式的: 字体: 12 磅
带格式的: 缩进: 首行缩进: 0.5 字符
带格式的: 字体: 12 磅
带格式的: 缩进: 首行缩进: 0.5 字符
带格式的: 字体: 12 磅

Table 2. Summary of aerosol species, analytical methods, measurement uncertainties and the method detection limits (MDLs).

Species	Analytical methods	Uncertainties	MDLs
Water soluble ions	Ion chromatography	3.5 - 7.0%	3 - 20 μg L^{-1}
Trace elements	ICP-OES	10.3 - 18.5%	-
OC, EC	Thermal-Optical Carbon Analyzer	<12%	30 - 80 ng m^{-3} for OC and 30 ng m^{-3} for EC (Mirante et al., 2014)
WSOC	TOC analyzer	3.4 - 6.0%	5.0 μg L^{-1}
PAH	GC-MS	20%	2 - 5μg L^{-1}
OM/OC ratio	SP-AMS	6% (Aiken et al., 2008)	-
WSOA	SP-AMS,TOC	6.9 - 8.5%	-

带格式的: 字体: 12 磅

Table 3. Summary of the mean concentrations (with one standard deviation) and mass fractions for ~~the~~ $PM_{2.5}$ and all quantified components in four seasons and the whole sampling period, respectively.

Species (μg m^{-3})	Spring	Summer	Fall	Winter	Annual
$PM_{2.5}$	**106.0±24.4**	**80.9±37.7**	**103.3±28.2**	**126.9±50.4**	**108.3±40.8**
WSIIs	**66.5±17.2**	**35.0±20.2**	**51.0±17.2**	**66.8±23.6**	**56.4**±22.9
Sulfate	17.3±4.8	15.8±9.8	17.2±6.2	18.7±7.6	17.5±7.1
Nitrate	26.4±8.7	6.8±6.2	17.0±9.0	24.1±11.8	19.3±11.6
Ammonium	14.8±4.2	8.2±4.3	11.2±3.2	13.1±3.7	12.0±4.2
Other ions	8.0±2.3	4.2±2.9	5.6±1.5	10.9±3.4	7.6±3.7
% of $PM_{2.5}$	62.~~6~~7±4.9	~~41.1~~43.2±7.4	49.~~0~~3±8.5	~~50.4~~52.6±7.3	52.1±9.7
TC	**16.0±3.3**	**12.1±1.6**	**21.0±11.8**	**22.3±8.6**	**19.2±9.3**
OC	11.2±2.6	7.9±0.8	13.2±7.8	18.3±8.1	13.8±7.5
EC	4.8±0.9	4.2±1.2	7.7±4.5	4.0±0.9	5.4±3.2
% of $PM_{2.5}$	15.~~3~~0±2.5	~~17.5~~15.0±6.5	~~19.7~~20.3±8.2	~~20.1~~17.6±3.3	~~18.1~~17.8±6.1
OA	**~~17.8±3~~18.9±~~4.1~~**	**~~12.9~~14.0±1.~~24~~**	**~~20.0~~21.6±11.~~69~~**	**~~29.6~~31.2±11.~~49~~**	**~~21.8±11~~23.3±9.0**
WSOA	~~13~~14.1±~~2.8~~3.0	~~11.0~~12.1±2.~~24~~	~~14.1±~~15.6~~.5~~±6.6	~~23.4~~25.1±8.~~0~~6	~~16.7±7.9~~18.1±6.1
WIOA	4.8±2.6	1.9±1.8	5.9±7.2	6.1±10.6	5.2±7.6
% of $PM_{2.5}$	17.~~1~~8±3.~~0~~2	~~19.0±7.~~18.2±8.4	~~18.7~~20.9±8.~~1~~3	~~23.9±5.5~~24.6±6.3	~~20.1±7.0~~21.5±6.8
PAHs (ng m^{-3})	**41.42±24.7**			**140.25±60.2**	
Trace elements			**2.77±1.15**	**6.38±3.14**	
OA+EC+WSIIs	**~~89.1±20.9~~90.2±21.0**	**~~52~~53.2±2~~1.5~~6**	**~~81.5~~83.1±29.6***	**~~106.8±35.9~~108.4±36.3***	**~~83.7±32~~85.1±27.9**
% of $PM_{2.5}$	**~~84.2~~85.1±5.**	**65.~~9±8~~±5.**	**~~78.9±14.9~~80.**	**~~84.2±11.7~~85.**	**~~77.3~~78.6±1**

带格式的: 字体: 12 磅
带格式的: 字体: 12 磅
带格式的: 字体: 12 磅
带格式的: 字体: 12 磅
带格式的: 字体: 加粗

	~~5~~6	4~~.8~~	4±15.0*	4±12.9*	1.6

*These values also include contributions from trace elements.

Table ~~3~~4. Mean concentration (ng m^{-3}) and mass fractions (%) of individual PAH to the total PAHs.

PAH compounds	Number of rings	Molecular formula and molecular weight (MW)	**Winter**		**Spring**	
			Conc. (ng m^{-3})	% of total	Conc. (ng m^{-3})	% of total
NaP	2-rings	$C_{10}H_8$,128	10.12	7.22	2.60	6.28
Acy		$C_{12}H_8$,152	0.16	0.12	0.08	0.20
Ace		$C_{12}H_{10}$,154	0.15	0.11	0.34	0.83
Flu	3-rings	$C_{13}H_{10}$,166	1.19	0.85	1.70	4.11
Phe		$C_{14}H_{10}$,178	3.54	2.52	3.24	7.83
Ant		$C_{14}H_{10}$,178	0.46	0.33	0.54	1.31
Flua		$C_{16}H_{10}$,202	8.05	5.74	2.57	6.21
Pyr		$C_{16}H_{10}$,202	8.93	6.37	2.43	5.87
BaA	4-rings	$C_{18}H_{12}$, 228	11.6	8.27	1.88	4.53
Chr		$C_{18}H_{12}$, 228	15.41	11.0	4.32	10.43
BbF+BjF		$C_{20}H_{12}$, 252	12.19	8.69	3.89	9.39
BkF		$C_{20}H_{12}$, 252	5.58	3.98	1.87	4.50
BaP	5-rings	$C_{20}H_{12}$, 252	10.33	7.37	3.43	8.29
BeP		$C_{20}H_{12}$, 252	12.08	8.61	2.42	5.83
DBA		$C_{22}H_{14}$, 278	2.53	1.8	0.42	1.02
InP	6-rings	$C_{22}H_{12}$, 276	20.74	14.8	5.23	12.62
BghiP		$C_{22}H_{12}$, 276	17.18	12.3	4.46	10.76

LMW-PAHs	2-3 rings	15.62	11.1	8.50	20.6
MMW-PAHs	4-rings	43.99	31.4	11.20	27.0
HMW-PAHs	5-6 rings	80.63	57.5	21.72	52.4
ΣPAHs		140.25	100.0	41.42	100.0

1127

Table ~~4~~5. Cross-correlation coefficients (*r*) of the measured concentrations of the PAH ~~speciesand~~species and ratios of the mean concentrations between these species from GC-MS (bold) and SP-AMS (itlaic).

PAHs	$C_{16}H_{10}$	$C_{18}H_{12}$	$C_{20}H_{12}$	$C_{22}H_{12}$	Ratio (GC)	Ratio (SP-AMS)
$C_{16}H_{10}$	1	*-0.250*	*-0.062*	*-0.140*	$\mathbf{C_{16}H_{10}/C_{16}H_{10}=1}$	$C_{16}H_{10}^{+}/C_{16}H_{10}^{+}=1$
$C_{18}H_{12}$	**0.952**	**1**	*0.572*	*0.528*	$\mathbf{C_{16}H_{10}/C_{18}H_{12}=0.84}$	$C_{16}H_{10}^{+}/C_{18}H_{12}^{+}=0.43$
$C_{20}H_{12}$	**0.936**	**0.994**	1	*0.771*	$\mathbf{C_{16}H_{10}/C_{20}H_{12}=0.36}$	$C_{16}H_{10}^{+}/C_{20}H_{12}^{+}=0.56$
$C_{22}H_{12}$	**0.925**	**0.986**	**0.993**	1	$\mathbf{C_{16}H_{10}/C_{22}H_{12}=0.35}$	$C_{16}H_{10}^{+}/C_{22}H_{12}^{+}=1.17$

$C_{16}H_{10}$: Flua+Pyr; $C_{18}H_{10}$: BaA+Chr; $C_{20}H_{12}$: BbF+BjF+BkF+BaP+BeP;
$C_{22}H_{12}$: BghiP+InP+DBA

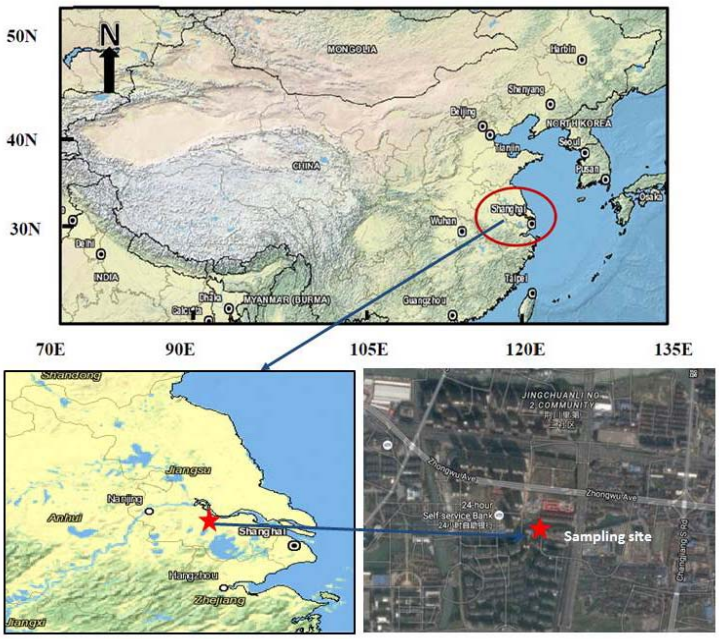

Figure 1. Schematic map of the sampling site~~,~~ and its surroundings ~~and location~~.

带格式的: 缩进: 首行缩进: 0 字符

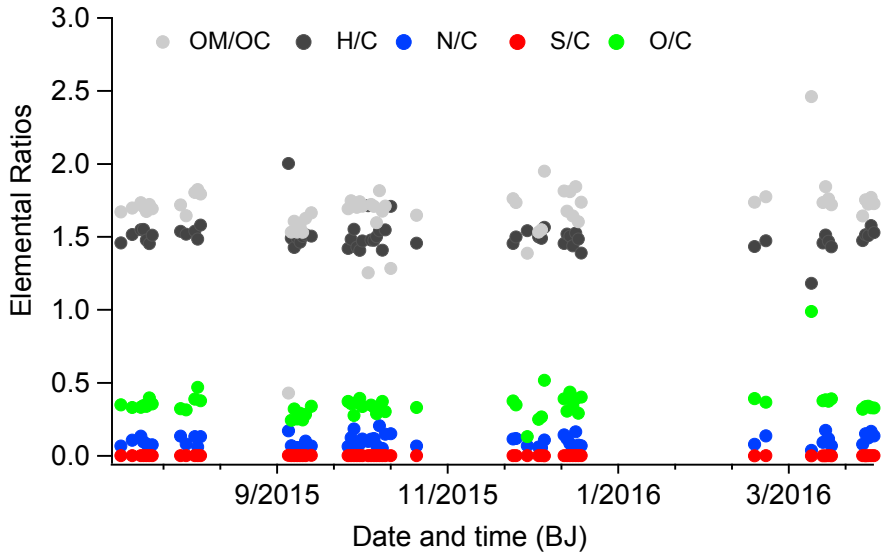

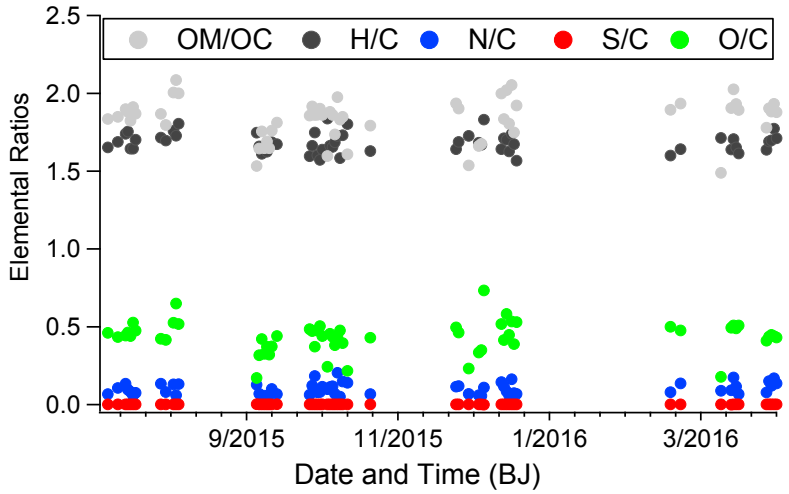

Figure 2. The atomic elemental ratios for the water-soluble organic ~~matter~~aerosols (WSOA) determined by the SP-AMS.

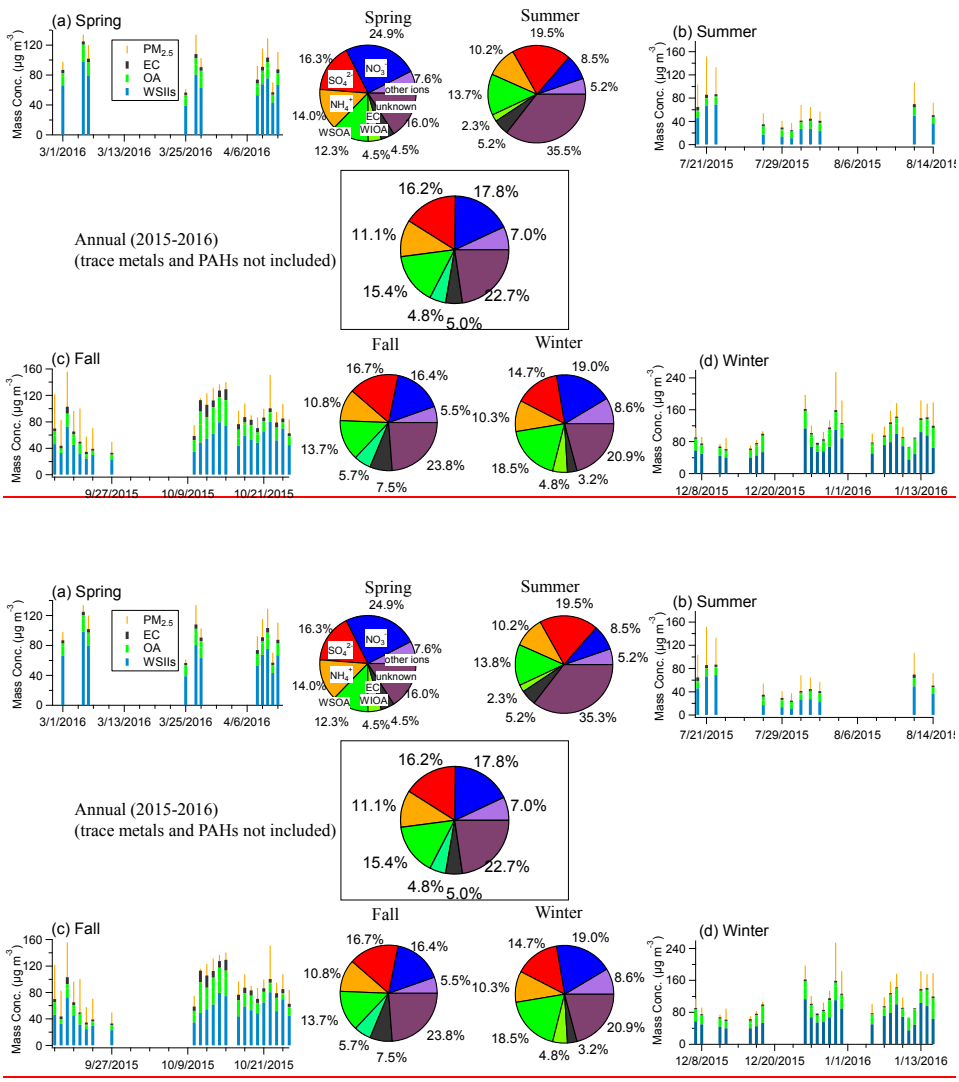

Figure 3. Reconstructed mass (= OA~~+~~ + EC~~+~~ + WSIIs) *vs.* $PM_{2.5}$ mass from gravimetric measurement ~~($PM_{2.5}$)~~ in (a) ~~sping~~spring, (b) summer, (c) fall, (d) winter, and annual. Corresponding pie charts show the mass percentages of different species to the $PM_{2.5}$ mass (trace elements and PAHs are not included due to sample limitations).

带格式的: 字体: 倾斜

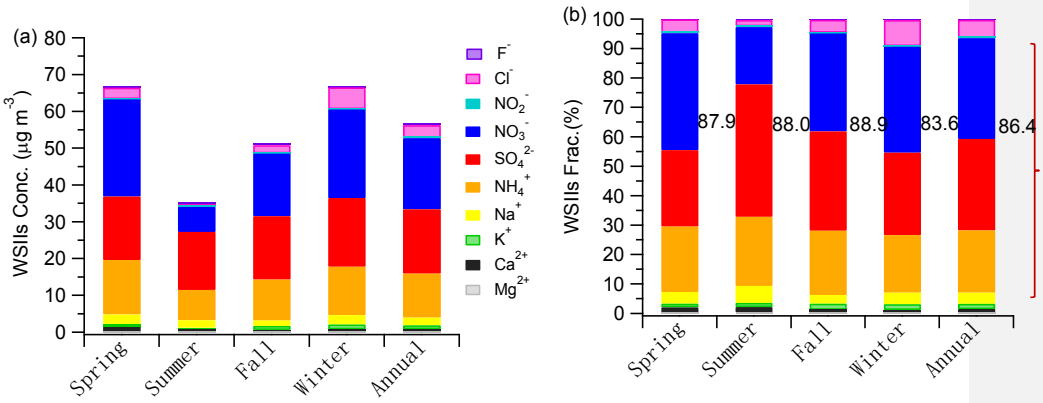

Figure 4. (a) Seasonal variations of average mass concentrations and (b) mass fractional contributions of WSIIs in $PM_{2.5}$ in Changzhou during 2015-2016. The values marked in (b) are the fractions of three ~~major~~most abundant ions (NO_3^-~~+~~+ SO_4^{2-}~~+~~+ NH_4^+) to the total WSIIs.

带格式的: 两端对齐

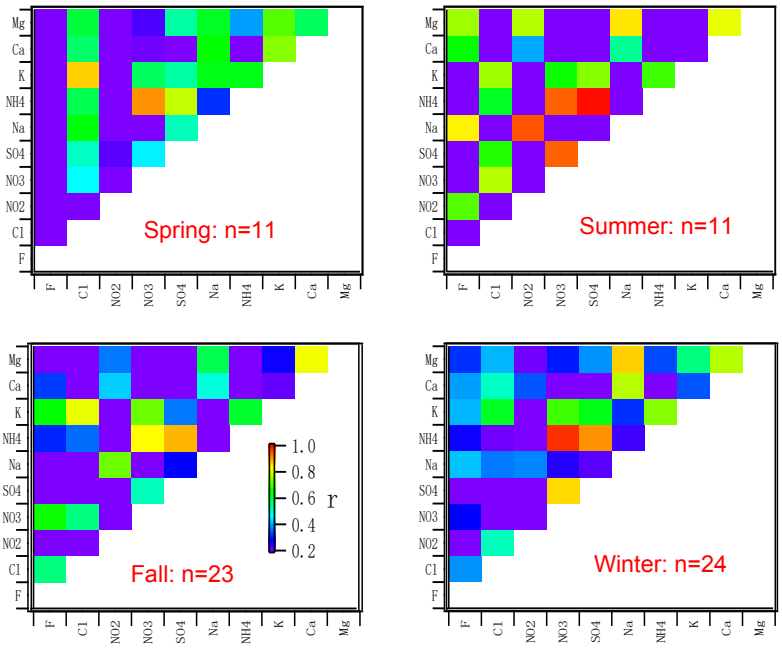

Figure 5. Image plots showing the cross correlation coefficients (*r*) between water-soluble ions in $PM_{2.5}$ in four seasons~~. Boxes are~~ (colored by ~~correlations (~~*r*).

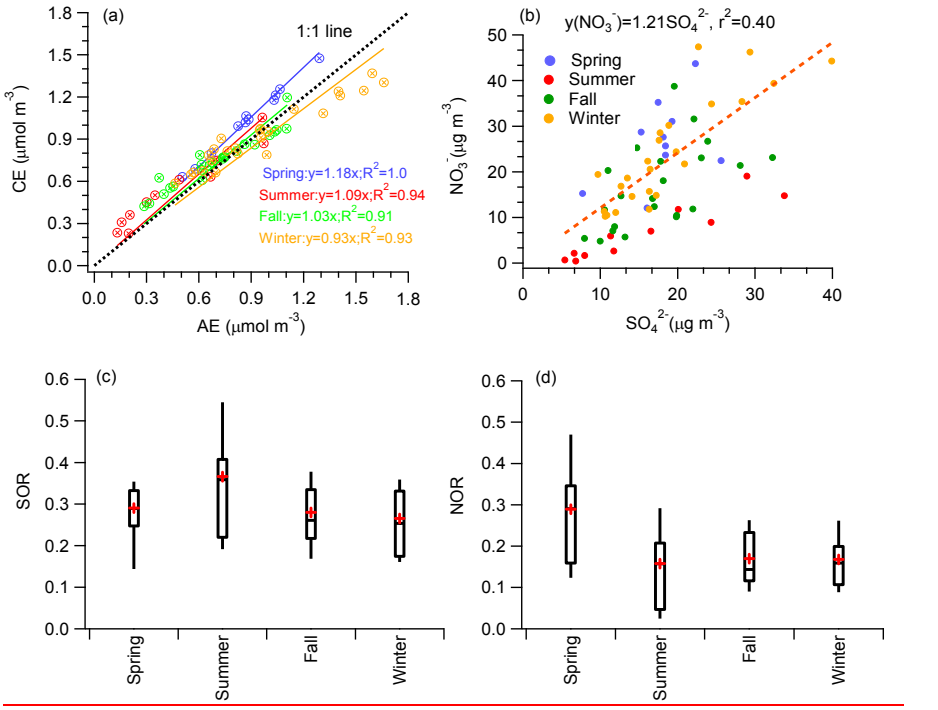
(a)
1:1 line
CE (μmol m-3)
AE (μmol m-3)
Spring:y=1.18x;R2=1.0
Summer:y=1.09x;R2=0.94
Fall:y=1.03x;R2=0.91
Winter:y=0.93x;R2=0.93
(b)
y(NO3-)=1.21SO4 2-, r2=0.40
Spring
Summer
Fall
Winter
NO3- (μg m-3)
SO4 2- (μg m-3)
(c)
SOR
Spring
Summer
Fall
Winter
(d)
NOR
Spring
Summer
Fall
Winter

1165

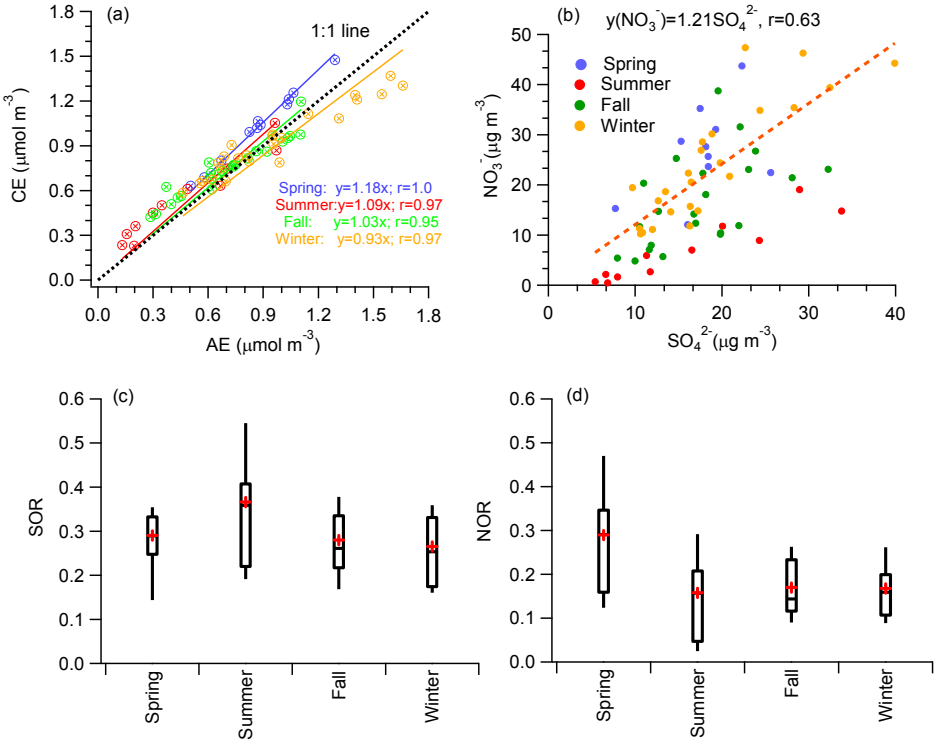
(a)
1:1 line
CE (μmol m-3)
AE (μmol m-3)
Spring: y=1.18x; r=1.0
Summer:y=1.09x; r=0.97
Fall: y=1.03x; r=0.95
Winter: y=0.93x; r=0.97
(b)
y(NO3-)=1.21SO4 2-, r=0.63
Spring
Summer
Fall
Winter
NO3- (μg m-3)
SO4 2- (μg m-3)
(c)
SOR
Spring
Summer
Fall
Winter
(d)
NOR
Spring
Summer
Fall
Winter

1166

Figure 6. (a) Scatter plots of molar concentrations of cations *vs.* anions, (b) scatter plots of NO_3^- *vs.* SO_4^{2-} concentrations, (c-d) SOR and NOR value during four seasons. In (a), the dashed line refers to 1:1 line. In (b), the dashed line was the averaged fitted line, representing NO_3^-/SO_4^{2-} ratio during the entire period. Data in different ~~season~~seasons are shown by different colors for comparison. Linear regression equations were also presented. In (c-d), the crosses represent the mean, the middle bars represent the median, the top and bottom of the box represents the 75^{th} and 25^{th} percentile, respectively, and the top and bottom whiskers represent the 90^{th} and 10^{th} percentile, respectively.

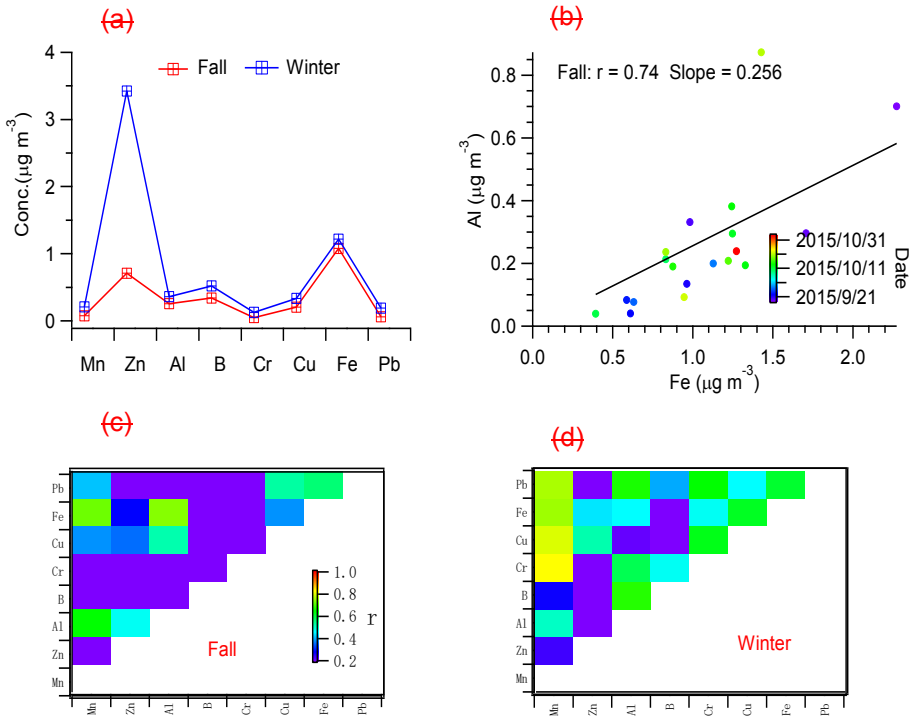

带格式的: 字体: 倾斜

带格式的: 字体: 倾斜

带格式的: 上标

带格式的: 上标

带格式的: 上标

带格式的: 上标

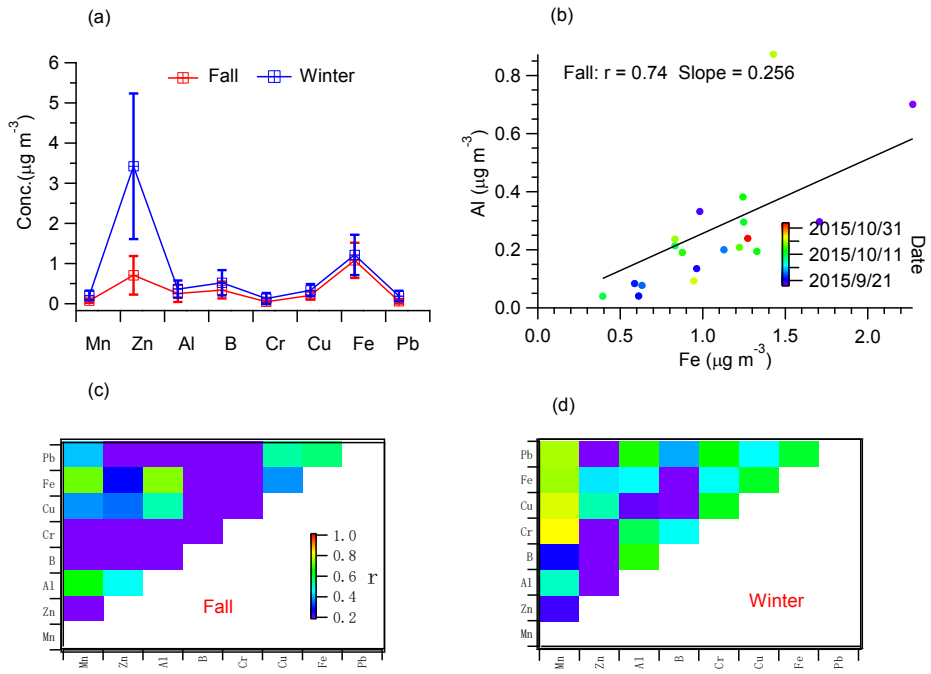

Figure 7. (a) Mean mass concentrations of trace elements determined for fall and winter~~,~~ (error bar represents the measurement uncertainty), (b) ~~Scatter~~scatter plots of Al ~~and~~*vs.* Fe in fall, and (c-d) cross-correlation coefficients (*r*) among different trace elements in fall and winter, respectively~~,~~ (colored by *r*).

1184

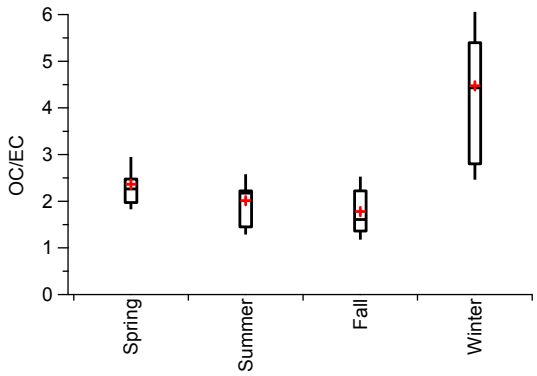

1185

1186 Figure 8. Average OC/EC ratios measured in four seasons (symbols of the box plots are the

1187 same as described in Figure 6.)

1188

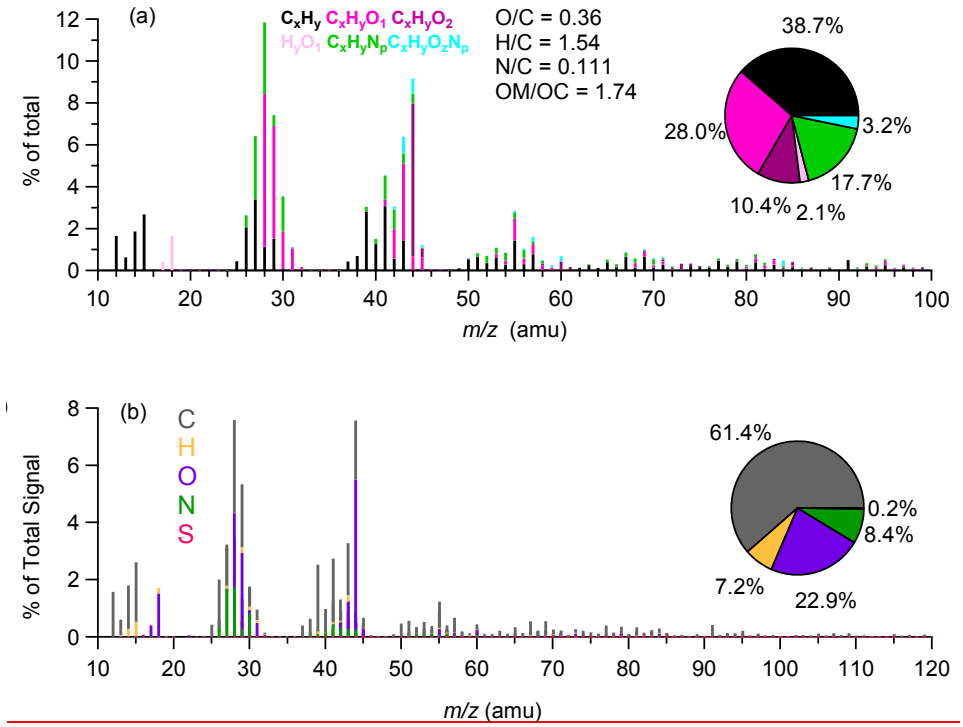

1189

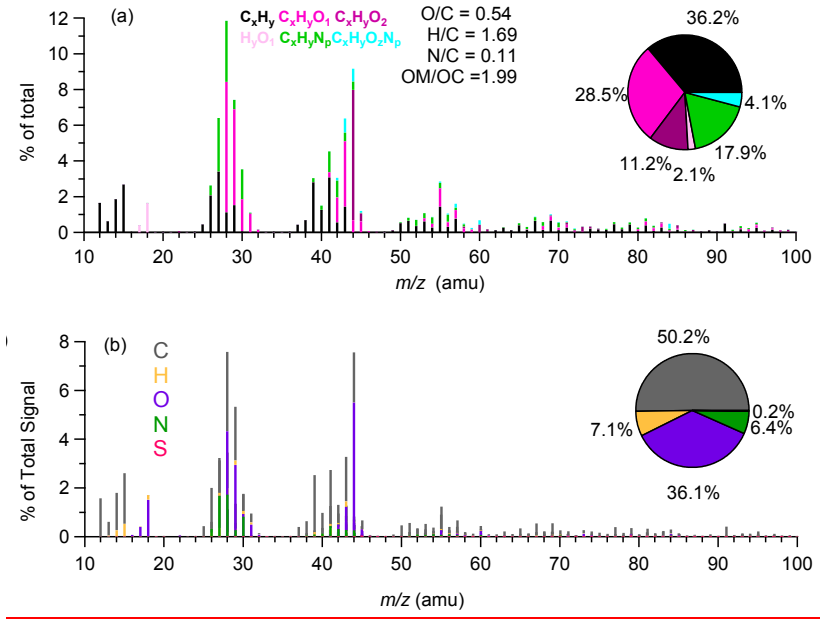

1190

1191 Figure 9. (a) High-resolution mass spectral profile of the WSOA measured by the SP-AMS
1192 (Mass spectrum is classified and colored by six ion families; pie chart shows the mass

contributions of each ion family to the total MS), (b) Average mass spectrum classified by five elements (C, H, O, N, and S) (inset pie chart shows mass contributions of the five elements, respectively).

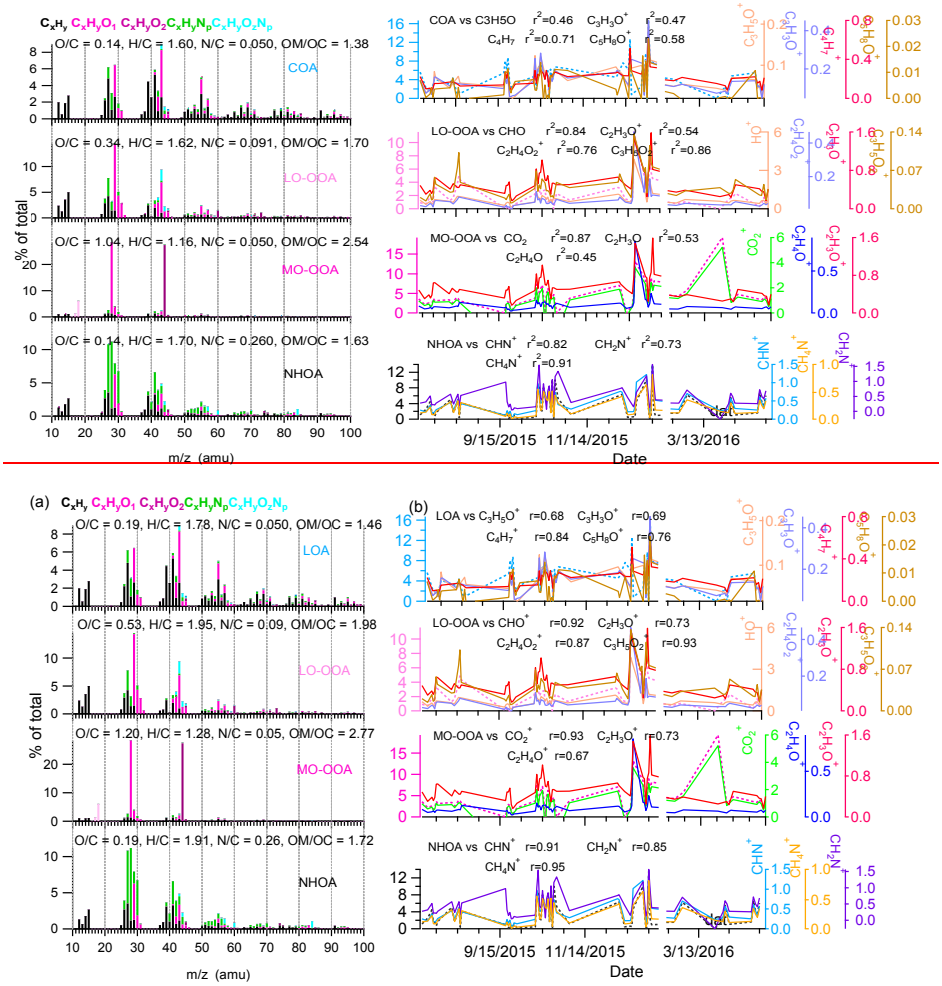

Figure 10. (a) High-resolution mass spectra of nitrogen-enriched hydrocarbon-like OA (NHOA), ~~cooking related~~local primary OA (~~COA~~LOA), less-oxidized OA (LO-OOA) and more-oxidized OA (MO-OOA) separated by the PMF analyses, colored by six ion categories, (b) time series of the four WSOA factors, and corresponding tracer ions.

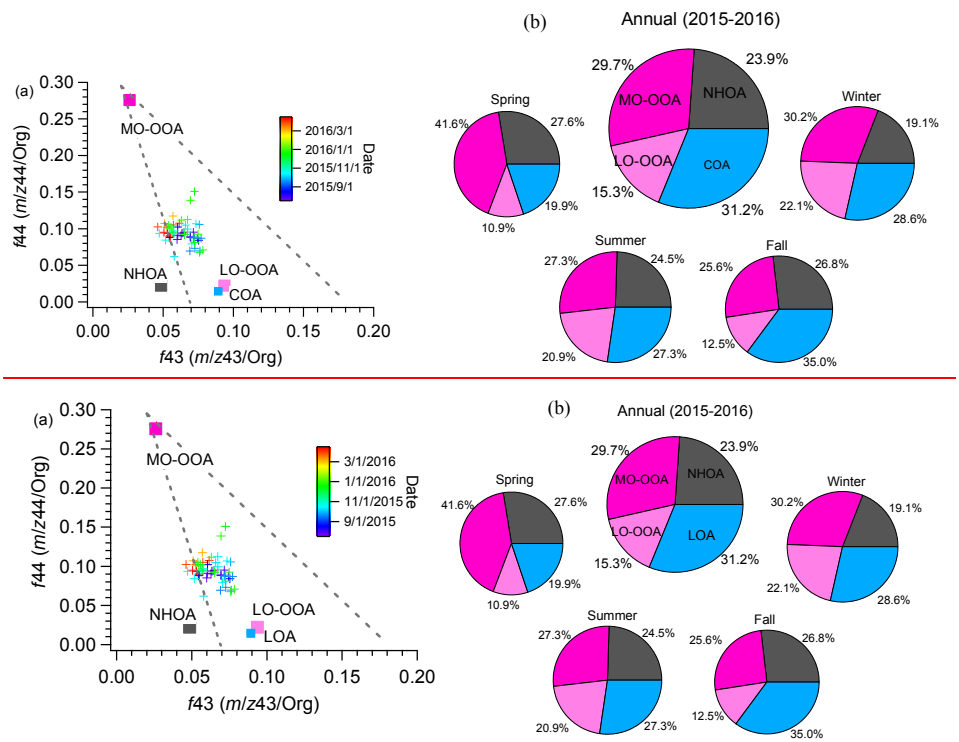

Figure 11. (a) Triangle plot of *f*44 *vs.* *f*43 for all WSOA, and the four WSOA factors identified by the PMF analyses, (b) pie charts of the mass contributions of four WSOA factors to the total WSOA in four seasons and the whole sampling period.

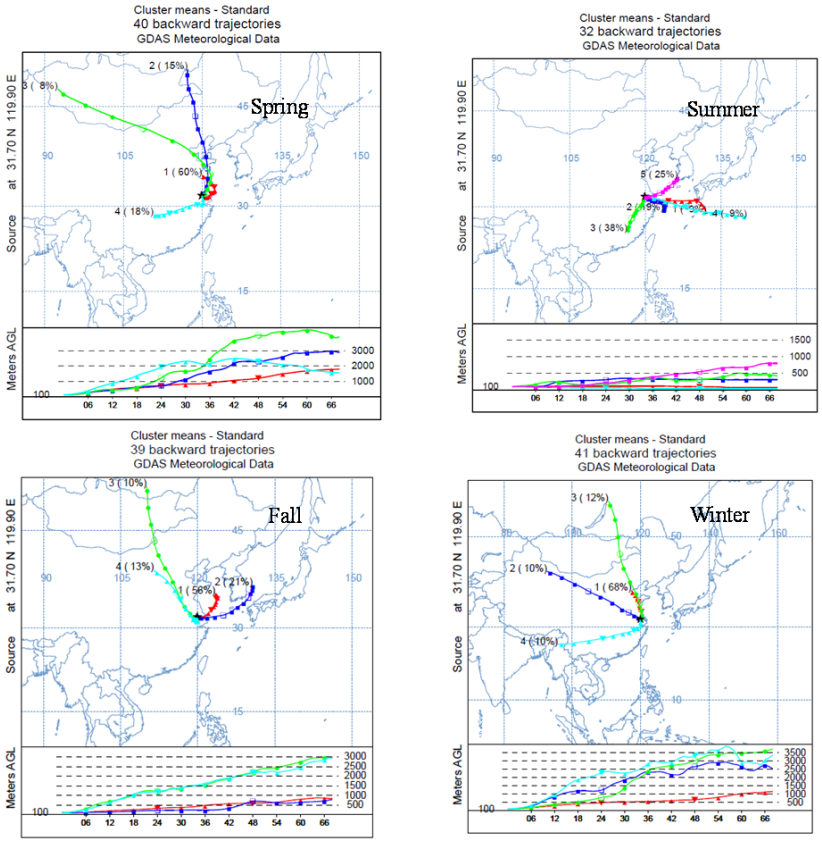

Figure 12. Air mass back trajectories across four seasons during the sampling period.

带格式的: 居中